

UNCLASSIFIED

AD NUMBER
AD921249
NEW LIMITATION CHANGE
TO Approved for public release, distribution unlimited
FROM Distribution authorized to U.S. Gov't. agencies only; Test and Evaluation; JUL 1974. Other requests shall be referred to Naval Weapons Lab., Dahlgren, VA.
AUTHORITY
UNNSWC ltr 11 Sep 1975

THIS PAGE IS UNCLASSIFIED

THIS REPORT HAS BEEN DELIMITED
AND CLEARED FOR PUBLIC RELEASE
UNDER DOD DIRECTIVE 5200.20 AND
NO RESTRICTIONS ARE IMPOSED UPON
ITS USE AND DISCLOSURE.

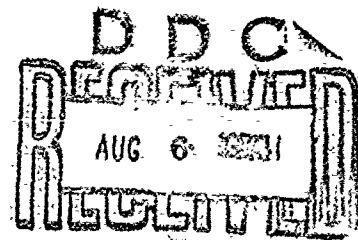
DISTRIBUTION STATEMENT A

APPROVED FOR PUBLIC RELEASE;
DISTRIBUTION UNLIMITED.

NWL TECHNICAL REPORT TR-3164
JULY 1974

CRITICAL EVALUATION AND STRESS ANALYSIS OF THE 5"/54 HI-FRAG PROJECTILE

Robert A. Lindeman



U. S. NAVAL WEAPONS LABORATORY
DAHLGREN, VIRGINIA



Distribution limited to U. S. Gov't. agencies
only; Test and Evaluation; (7-74). Other
requests for this document must be referred
to the Commander, Naval Weapons Laboratory,
Dahlgren, Virginia 22448

NAVAL WEAPONS LABORATORY
Dahlgren, Virginia
22448

R. B. Meeks, Jr., Capt., USN
Commander

James E. Colvard
Technical Director

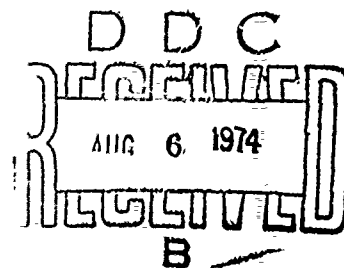
NWL TECHNICAL REPORT TR-3164
JULY 1974

CRITICAL EVALUATION AND STRESS ANALYSIS OF THE
5"/54 HI-FRAG PROJECTILE

By

ROBERT A. LINDEMAN

Product Engineering Division, Engineering Department
Naval Weapons Laboratory, Dahlgren, Virginia 22448



ACKNOWLEDGMENT

The author wishes to acknowledge the large number of people who have helped in the successful completion of this analysis. In particular, I have benefited from my many discussions with Dr. J. R. Thompson, Jr., Mr. J. E. Bennett, and Mr. J. C. Newquist.

I also wish to thank Mrs. A. D. Moore for typing this report.

This work was performed for the Munitions Division of the Surface Warfare Department under NAVORD Task No. 55-10/005/178-1 and 4, 20 July 1973.

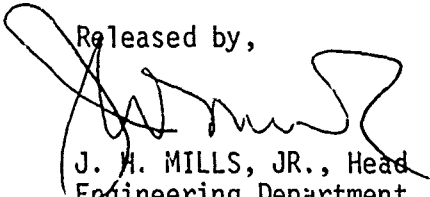
FOREWORD

The following report gives the details of the stress analysis and critical flaw size calculations for the 5"/54 HI-FRAGMENTATION Projectile. The various assumptions which are made in the analysis are discussed and the errors associated with these assumptions are estimated.

The report provides the necessary theory and its application to a specific projectile. The results are presented and discussed for the specific projectile designers. The methodology is presented for those performing similar analyses. This material should serve as a basis for refining the approach in order to reduce the inherent uncertainties associated with this type of analysis.

This report has been reviewed by Mr. D. W. Culbertson, Head, Materials Branch and Mr. R. J. Arthur, Head, Product Engineering Division.

Released by,



J. H. MILLS, JR., Head
Engineering Department

ABSTRACT

This report presents a detailed analysis of the loading conditions to which the 5"/54 HI-FRAG Projectile is subjected. These loading conditions include the following: press fit, gun ramming and engraving, maximum acceleration upon gun launch, and stress relaxation or rebound upon exit from the barrel.

The analyses are based on finite element, analytical, and experimental results. Where applicable, various results are correlated to show their validity.

The analyses show that the joint region is the most highly stressed region in the projectile. The critical flaw size under 18,000 g's gun-launch loading conditions is about 0.028 by 0.28 inches for a sharp elliptical crack in the joint region at 0.006 inches radial interference.

TABLE OF CONTENTS

ACKNOWLEDGMENT	i
FOREWORD	ii
ABSTRACT	iii
INTRODUCTION	1
FINITE ELEMENT PROGRAM	3
5"/54 HI-FRAG PROJECTILE AND MATERIAL PROPERTIES	4
PRESS FIT RESIDUAL STRESSES.	8
RAMMING INTO BARREL.	14
GUNLAUNCH.	15
CRITICAL FLAW SIZE	26
REBOUND.	30
DISCUSSION	31
CONCLUSIONS AND RECOMMENDATIONS.	34
REFERENCES	35
APPENDIX A	A-1
APPENDIX B	B-1
APPENDIX C	C-1
APPENDIX D	D-1
APPENDIX E	E-1

INTRODUCTION

This report deals with the many and varied loading conditions to which the 5"/54 HI-FRAGMENTATION Projectile is subjected. Figure 1 shows a general sketch of this projectile. As shown in the figure, this projectile consists of two metal pieces joined by a press fit. The press fit sets up residual stresses in both pieces. In order to accurately determine these stresses a finite element program (ZPII) was used. This program is briefly described in the next section.

The joint experiences a tensile load when it is rammed into the gun. The joint must withstand this load to avoid slipping between the two pieces of the projectile.

Upon setback, the joint must transmit very large axial and circumferential loads. The circumferential load is caused by spin-up of the projectile. At the same time a large tensile hoop stress is generated which may cause crack propagation and brittle fracture.

As the projectile exits the muzzle the acceleration drops off very rapidly. This causes the stored elastic energy to go into stress waves and causes the projectile to ring at its natural frequency. At the same time, the aerodynamic drag changes and a slight deceleration may occur. This phenomenon is called rebound.

This report discusses all of the above loading conditions and attempts to evaluate the present design under each condition.

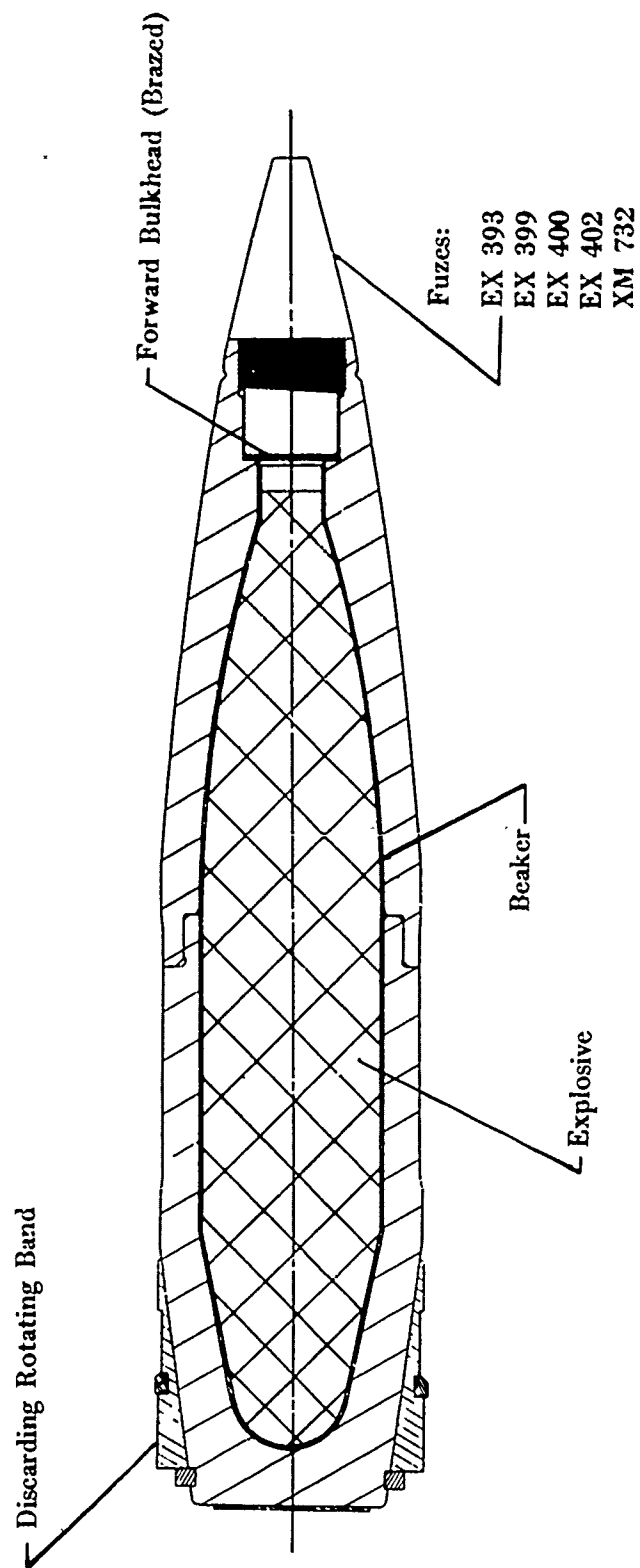


FIGURE 1. SCHEMATIC OF 5"54 HI-FRAG PROJECTILE

FINITE ELEMENT PROGRAM

The complex geometry in the joint region made an analytical analysis using Lamé equations impossible. To obtain a stress analysis at this region, an existing finite element program was modified to include the effects of interfering surfaces. The program, ZPII, is described in detail in reference (1). The following discussion is included to show the capabilities and limitations of the computer model.

The computer program performs a static stress analysis of axisymmetric bodies containing internal surfaces. These surfaces may initially be open, in contact, or interfering as in the case of press fits. Friction-free relative motion between the two surfaces is allowed.

The allowable loading conditions are pressure loaded edges, axial acceleration body forces, and direct nodal loads.

The major advantage in using this computer code for press or thermal fit analyses lies in the fact that only the geometry and material properties are needed as input. The interference pressure and equilibrium deformations are calculated by the program. This is far superior to previous methods in which either an interference pressure or the final equilibrium position of the two pieces at the interface had to be assumed, references (2) and (3).

The major limitations in ZPII for this analysis are the neglect of body forces due to angular velocity and acceleration, and the neglect of shear stresses along contact and interfering surfaces. An estimate of the errors is included in each case in which one of these is neglected.

5"/54 HI-FRAG PROJECTILE AND MATERIAL PROPERTIES

Figures 2 and 3 show the dimensions of the two pieces which constitute the 5"/54 HI-FRAG Projectile. These pieces enclose an explosive billet of PBXW-106.

The two pieces are manufactured with an allowable radial interference of .002 to .006 inches before knurling. The interference surface of the base is knurled which increases the radial interference. In a preceding design (the 5"/54 Improved Projectile), the after-knurling radial interference ranged from .0050 to .0135 inches, reference (4). However, the increased yield strength of the HI-FRAG Projectile (150 KSI versus 80 KSI) will probably lower this increase in interference. No data is presently available for the range of interferences for the HI-FRAG Projectile.

In order to obtain a naturally high fragmenting projectile, HF-1 steel heat treated to a nominal yield stress of 150 KSI was chosen for the projectile body. Analysis of the fragmentation properties of this steel is given in reference (5). A typical static (.05 in/min) stress strain curve, from reference (6), for this material is shown in Figure 4 along with the approximate curve used for the elastic plastic computer analysis.

With this heat treatment, HF-1 has an ultimate tensile strength of 198 KSI and a longitudinal K_{IC} value of $31.4 \text{ KSI } \sqrt{\text{in}}$ at 70°F. These values were obtained from projectiles produced at NWL. No data is presently available on contractor projectiles. Moreover, no transverse K_{IC} values have been obtained on any projectiles.

The explosive is a plastic bonded explosive. It is assumed that under large setback loads, the explosive behaves as a fluid.

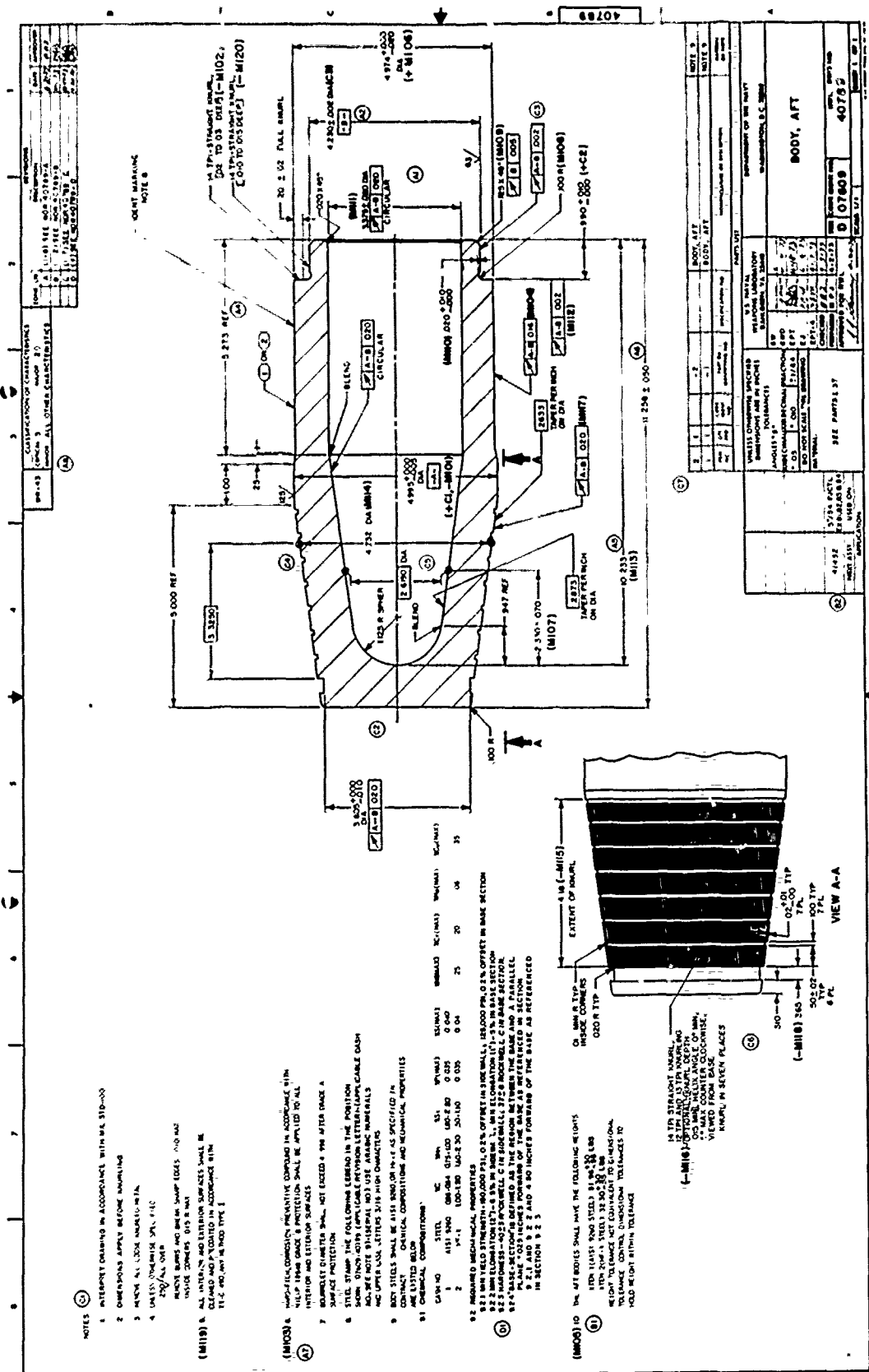


FIGURE 3.

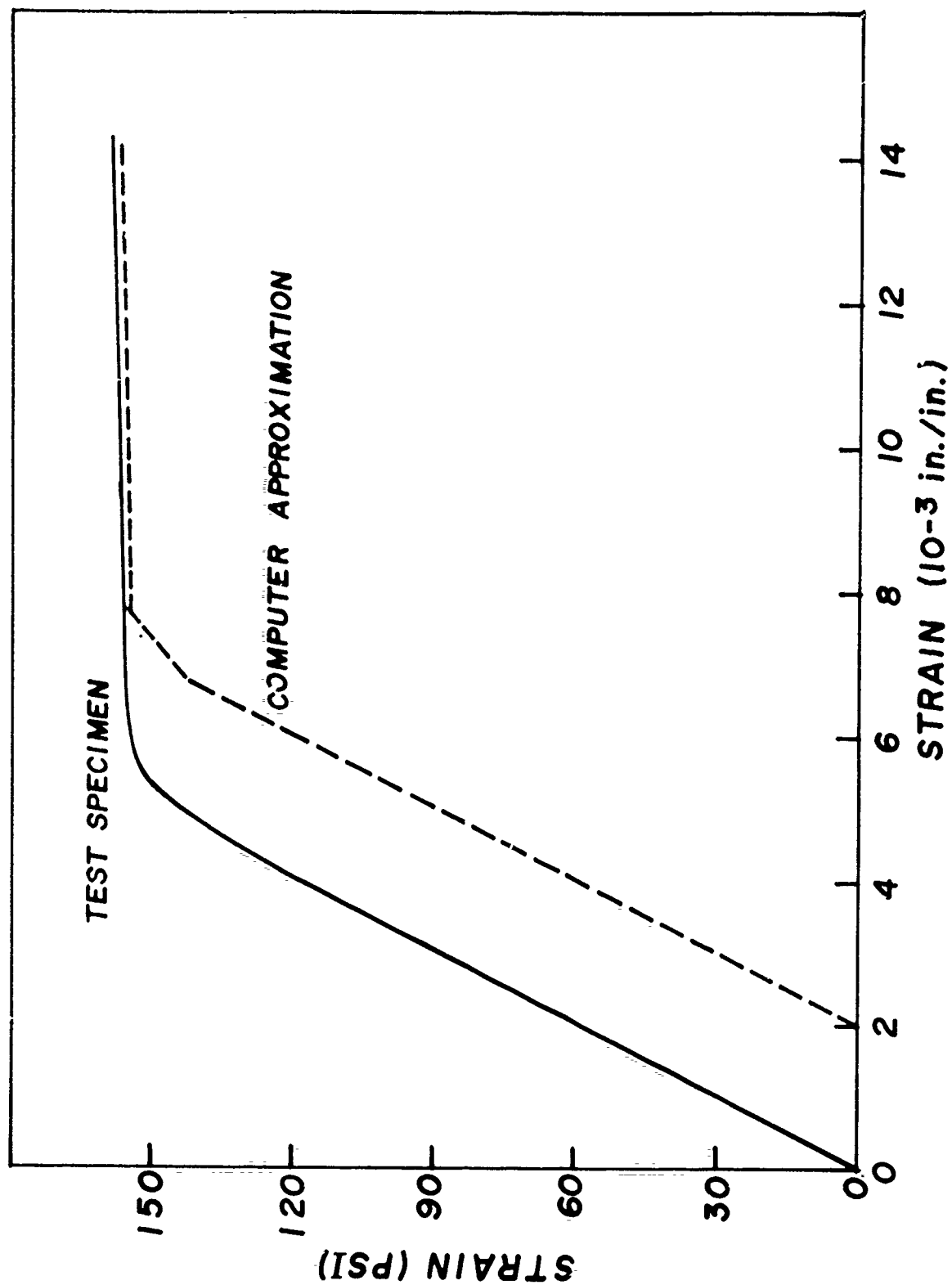


FIGURE 4. TYPICAL TENSILE STRESS-STRAIN CURVE FOR 150 KSI HF-1 STEEL AND THE COMPUTER APPROXIMATION USED IN THE ELASTIC-PLASTIC ANALYSIS

PRESS FIT RESIDUAL STRESSES

The joint region of the projectile was modeled by the finite element mesh shown in Figure 5. This model was used to evaluate the residual stresses set up by the press fit. Figures 6 and 7 show the radial and hoop stress contours for a .006 inch radial interference. Note that this is not the largest interference used in the HI-FRAG Projectile. As data concerning the maximum interference after knurling becomes available, these results will have to be extended to include the worst case.

The radial stress contours in Figure 6 show that the interference pressure varies from 9 to 25 KSI along the interface. This indicates that the assumption of uniform interference pressures made by previous authors, reference (2), is greatly in error. Figure 8 plots the interference pressure versus position along the joint. Also shown is the value obtained from the simple analytical press fit equations, reference (7).

Figure 7 shows that the nose experiences a large tensile hoop stress (positive sign) while the base experiences a large compressive stress (negative sign). At .006 inches interference, the maximum tensile stress is about 60 KSI.

This analysis assumes that the joint region remains elastic. To evaluate this assumption one must consider the effect of the knurling in the press fit. It was expected that the knurling would yield at a much lower pressure than the solid metal surface.

To provide data on the effect of knurling, several 5"/54 IMPROVED Projectiles which have a joint similar to the HI-FRAG Projectile were pressed together in the lab. By comparing the measured values of hoop strains at various locations around the joint with the computer strains given by the computer model, the effect of the knurling could be evaluated. These results are given in reference (4) with a brief analysis presented in Appendix A.

This study shows that the knurling in the IMPROVED joint exhibits a range in its behavior with an upper limit equivalent to a solid surface. Thus, the computer results should be considered as the upper limit or worst case under any given loading conditions. This allows the computer model to be used both in the evaluation of the projectile design and in the calculation of the critical flaw size.

Recall that shear stresses along the interference surface are neglected in this analysis. This shear stress has a maximum value equal to the product of the normal stress (interference pressure) and the coefficient of static friction (0.15). Thus, the shear stress for .006

MT FRAG JOINT MESH

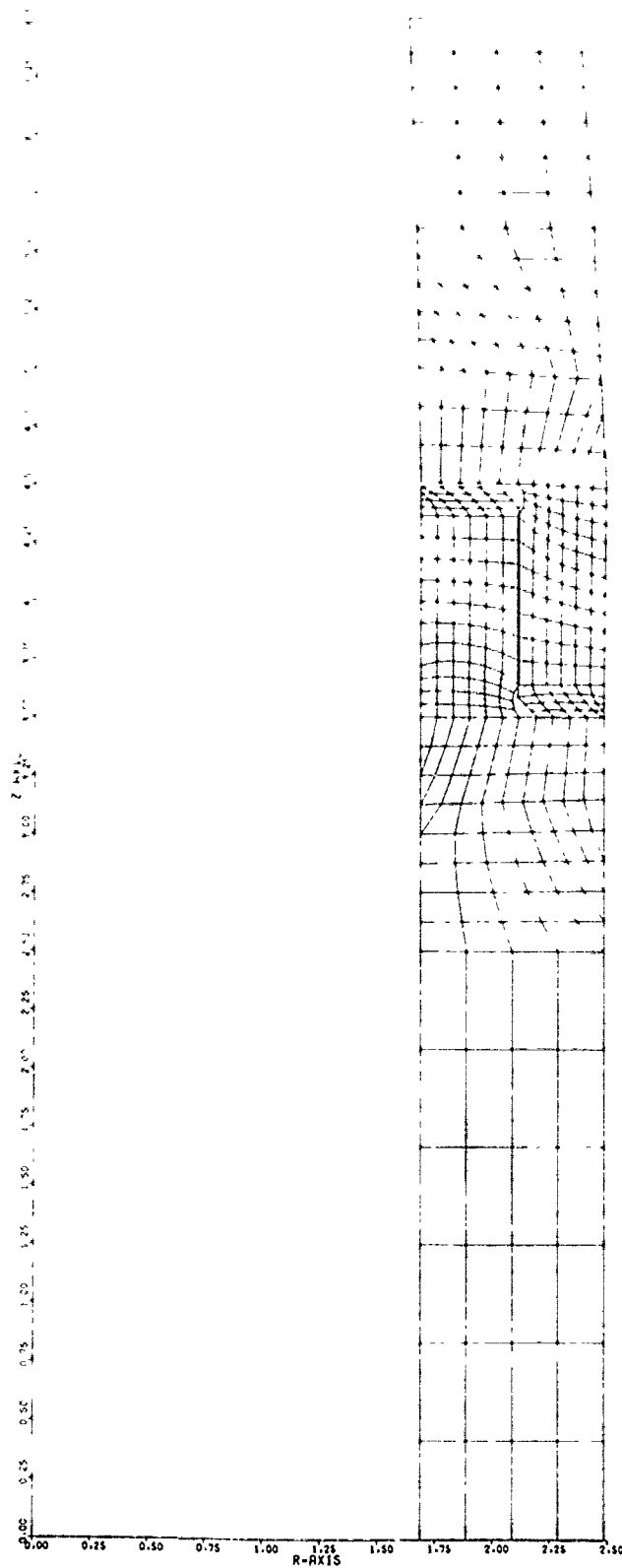


FIGURE 5. MESH USED FOR JOINT ANALYSIS

RADIAL STRESS CONTOURS (KSI)

HI-FRAG JOINT MESH

ELASTIC ANALYSIS AT 1g

$\delta = .006"$

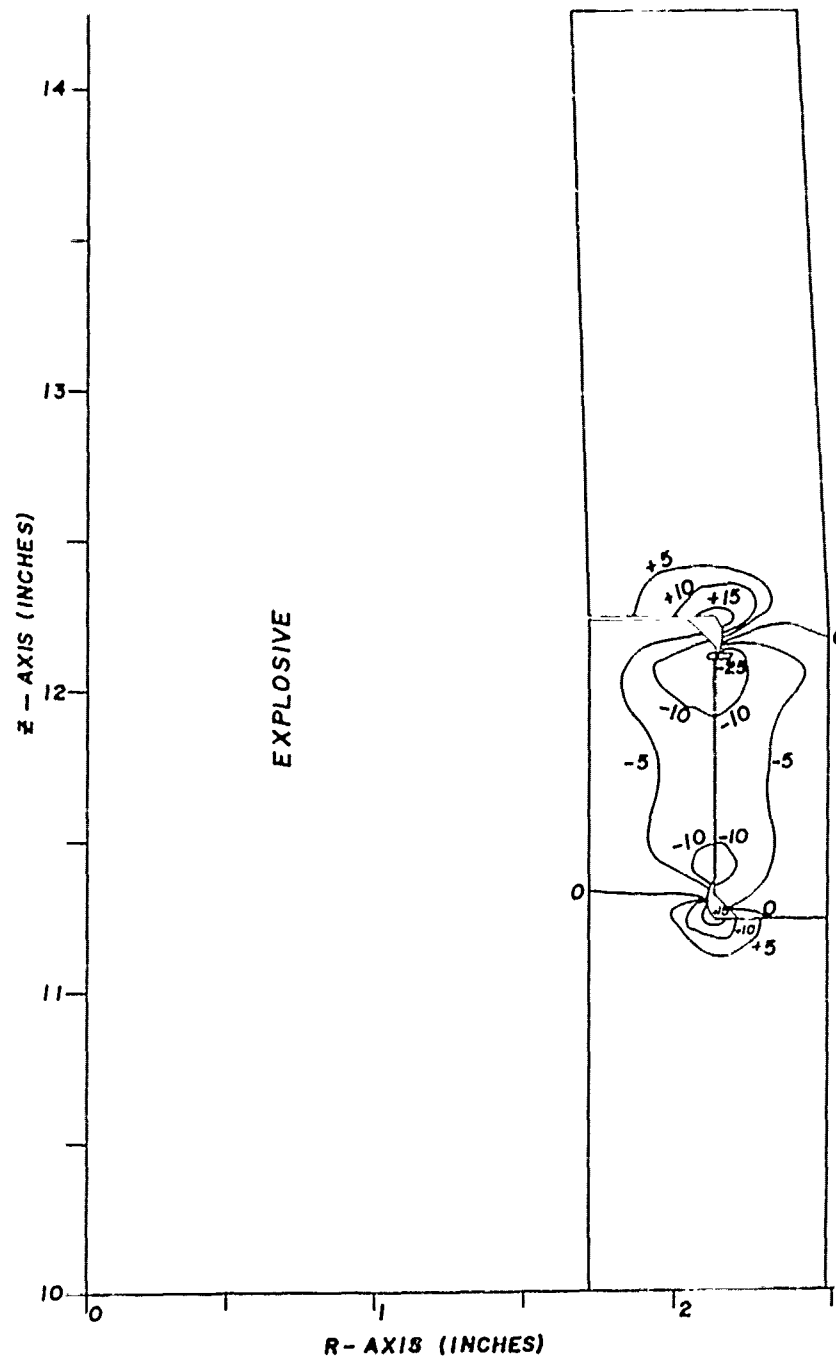


FIGURE 6. RADIAL STRESS CONTOURS DUE TO PRESS FIT

HOOP STRESS CONTOURS (KSI)
 HI-FRAG JOINT MESH
 ELASTIC ANALYSIS AT 1g
 $\delta = .006"$

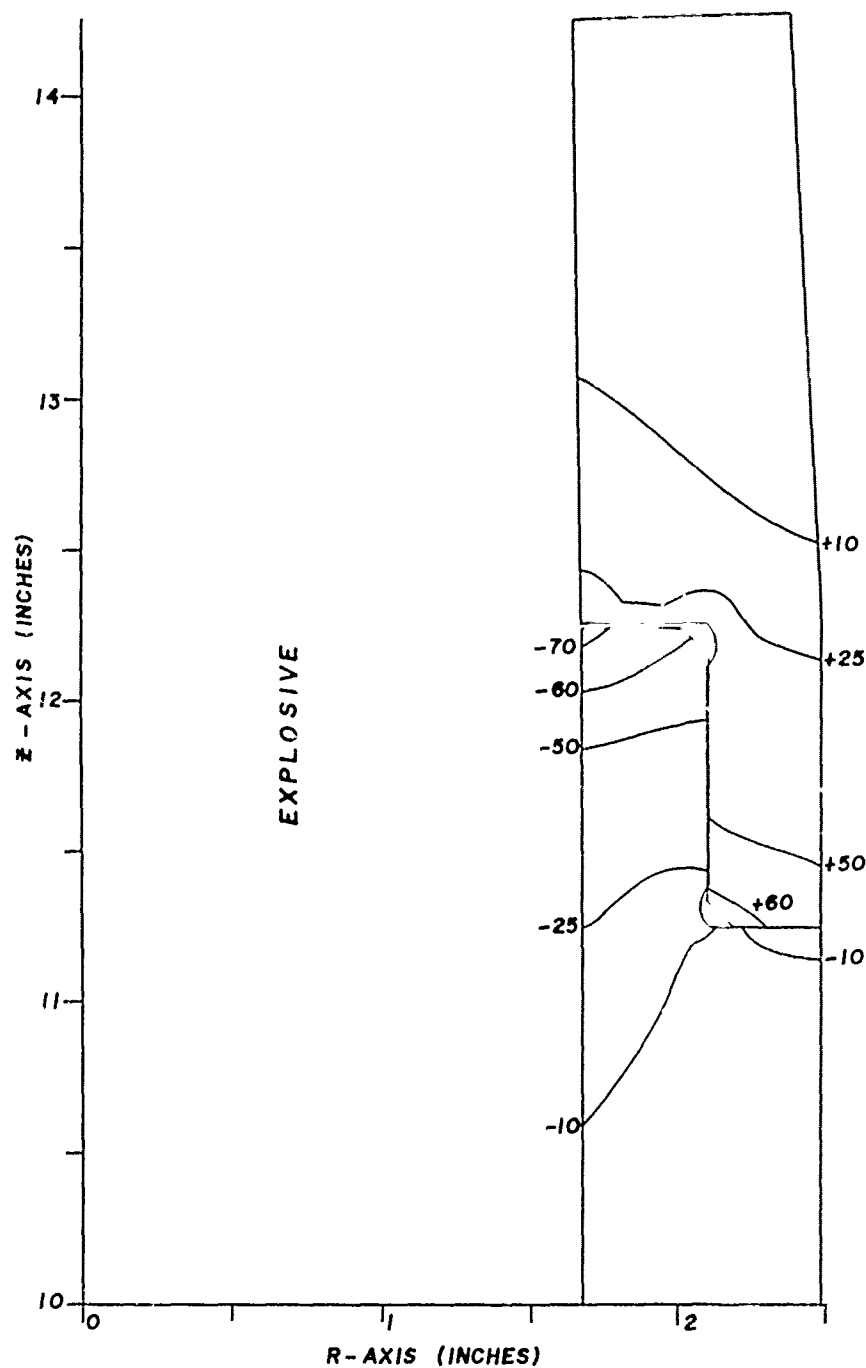


FIGURE 7. HOOP STRESS CONTOURS DUE TO PRESS FIT

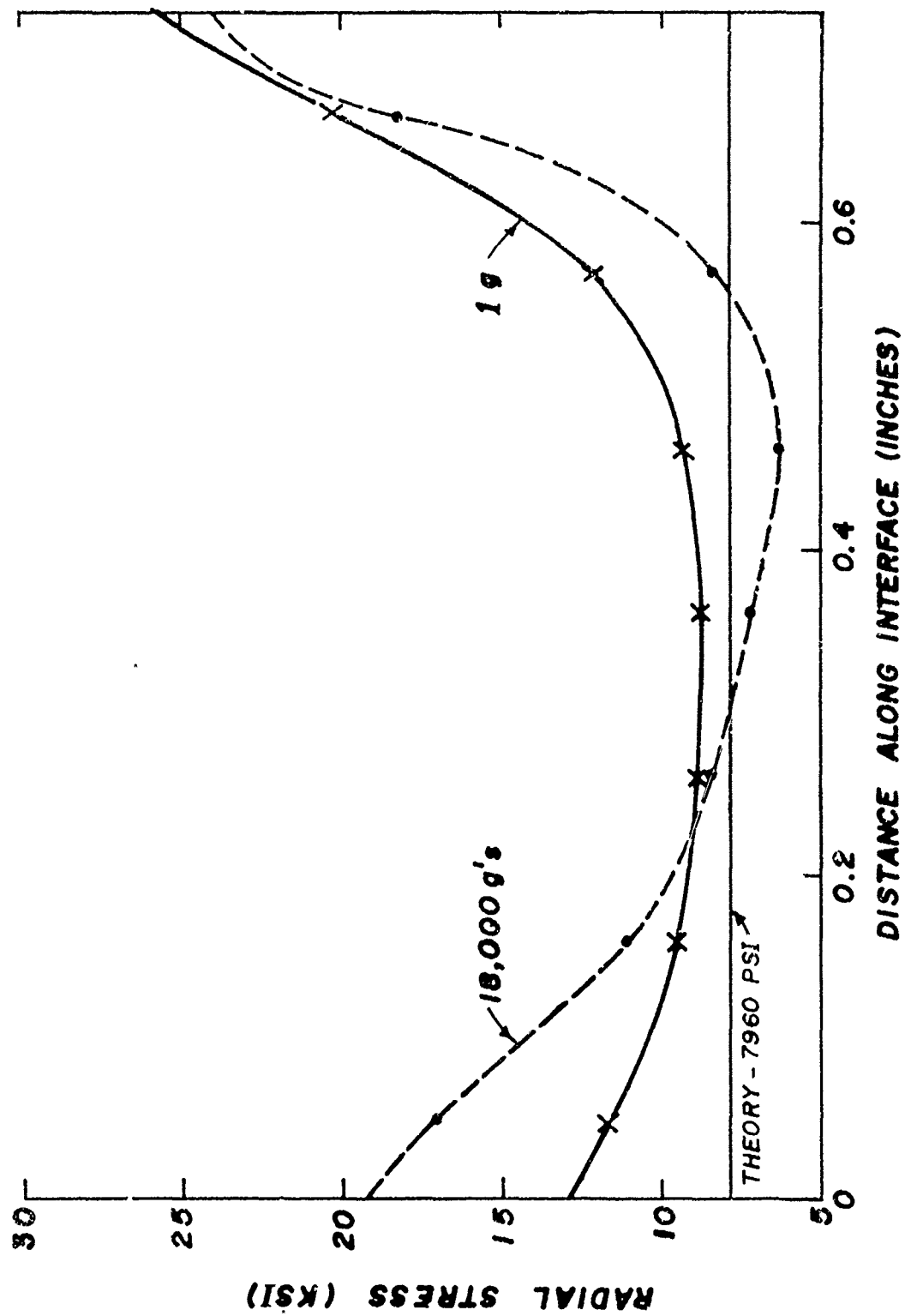


FIGURE 8. RADIAL STRESS VERSUS POSITION ALONG INTERFACE AT PRESS JOINT.

inch interference has a range of 1 to 4 KSI. This is a negligible contribution to the stress state when compared to the radial stress (9 to 25 KSI) and hoop stress (10 to 70 KSI). Moreover, Horger (8) reports an increase in press fit holding strength with time. This is probably due in part to the relaxation of the residual shear stresses at the interference surface. These stresses are directed so as to aid in separating the press fit.

RAMMING INTO BARREL

The maximum ram speed for the 5"/54 Projectile is 24 ft/sec. Since the projectile is stopped by the rotating band, the joint must transmit the axial force required to stop the nose, the fuze, and possibly the explosive billet (total weight of 37.8 lbs).

The maximum deceleration in ramming tests, reference (9), has been 250 g's for copper rotating bands and 70 g's for plastic bands. The force required to decelerate the nose, fuze, and explosive at 250 g's is 9,500 lbs. Up to the present time, the smallest tensile load which caused slip in the joint is 14,000 lbs for the IMPROVED Projectile (Appendix A).

However, the minimum interference after knurling for the IMPROVED Projectile was 0.005 inches. Based on a static coefficient of friction of 0.15, the computer model predicts a holding force for the HI-FRAG Projectile given by:

$$F = 2.80 \delta$$

where F = holding force (10^3 lbs)
 δ = radial interference (10^{-3} in).

Thus, a minimum radial interference of .0035 inches is required if a copper band is used. An interference of .002 inches will allow a deceleration of about 130 g's.

This is based on the average value of holding force. A worst case analysis based on present data gives a maximum deceleration of about 110 g's for a .002 inch radial interference.

GUNLAUNCH

A projectile may fail structurally either in a plastic mode or a brittle mode. Plastic failure occurs when sections of the projectile undergo such large plastic deformations that they can no longer transmit the applied load. For example, plastic deformation can greatly reduce the holding force of the joint. Brittle failure occurs when a flaw is stressed to a level where it propagates unstably.

This section presents the stress state and plastic deformations under gunlaunch conditions. Brittle failure will be considered in the next section.

The HI-FRAG Projectile will be subjected to a maximum acceleration in the range of 12,000 to 15,000 g's. However, since proof pressure would cause an acceleration of 18,000 g's, the projectile is being designed for 18,000 g's.

This analysis uses .006 inch radial interference. It is thus not the worst case but is useful in understanding the stress state of the projectile.

The computer model gives a static stress analysis. Appendix B considers the errors introduced by neglecting dynamic effects. This error analysis indicates that the dynamic effects due to acceleration body forces introduce an error less than 1%. However, there are two other sources of dynamic loads: shock loading due to the sonic coupling with the propellant, and side slap of the projectile against the interior of the bore. Reference (10) shows that the shock loading from the propellant decays in about 2 msec and therefore will not give a significant error at the time of maximum acceleration (8 msec). The dynamic effects due to side slap have never been measured. Thus, their effect is unknown.

Appendix C considers the errors introduced by neglecting angular velocity and acceleration. These errors are about 3%.

The loading conditions for the projectile are as follows:

- 1) A rotating band pressure of 63,000 psi;
- 2) A liquid model for the explosive PBXW-106 given by

$$P = \rho gh$$

where P = explosive pressure

ρ = explosive mass density

g = acceleration

h = distance below the top surface of the explosive;

3) A fuze pressure of 16,060 psi based on a 2.08 lb fuze.

These loading conditions are discussed in detail in Appendix D.

Using the mesh shown in Figure 9, an elastic stress analysis of the whole projectile at .005 inches radial interference was obtained. These results are shown in Figures 10 and 11.

Figures 10 and 11 show that the joint section is the critical region for this projectile. The joint has a maximum von Mises stress of over 175 KSI and a maximum tensile hoop stress of 58 KSI. Outside this region the maximum von Mises stress is 125 KSI which is below the yield strength of the material (150 KSI) and a maximum tensile hoop stress of 28 KSI.

To obtain a better analysis of the joint at 18,000 g's, the mesh shown in Figure 5 was used. The boundary conditions were compared to the analysis of the whole projectile to assure that no bending moments were being introduced or overlooked.

The elastic analysis at .006 inches radial interference is given in Figures 12 and 13. Since the axial stress is much larger than either the radial stress or hoop stress, the axial stress contours are very similar to the von Mises stress contours.

When the two pieces are pressed together, the bottom surface of the nose tilts with respect to the base as shown in Figure 14. At .006 inch interference, this tilt leaves a gap of .0005 inches at the outer surface. On setback this concentrates all of the axial load on the inside part of this contact surface until it deforms enough for the whole surface to come in contact. This is shown in Figure 12 by the large von Mises stress concentration at the inside corner of this contact surface.

The 0.0005 inch gap represents a tilt of 0.10° across the contact surface. This is much larger than the perpendicularity and flatness requirements for this surface (0.02°) and thus would be real if two solid surfaces were directly in contact. However, the base surface is knurled. It is expected that the knurling will distribute the axial load across the surface much more efficiently than the computer program predicts.

No quantitative data is presently available on the effect of this knurling. Since the knurling on the contact surface is 0.02 to 0.03 deep and the knurling on the interference surface is 0.010 to 0.015 deep, one might expect the knurling on the contact surface to yield at a lower stress than the interference knurling. This yielding effect may be partially offset if the height of the knurling is higher on the inside of this surface than the outside.

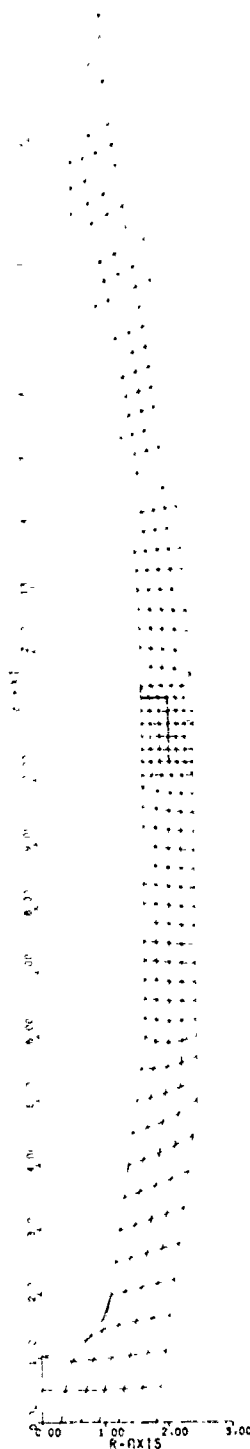


FIGURE 9. MESH USED FOR PROJECTILE ANALYSIS

HOOP STRESS CONTOURS (KSI)
 HI-FRAG INTERFERENCE FIT
 ELASTIC ANALYSIS 18,000 g's
 $\delta = 0.005^\circ$

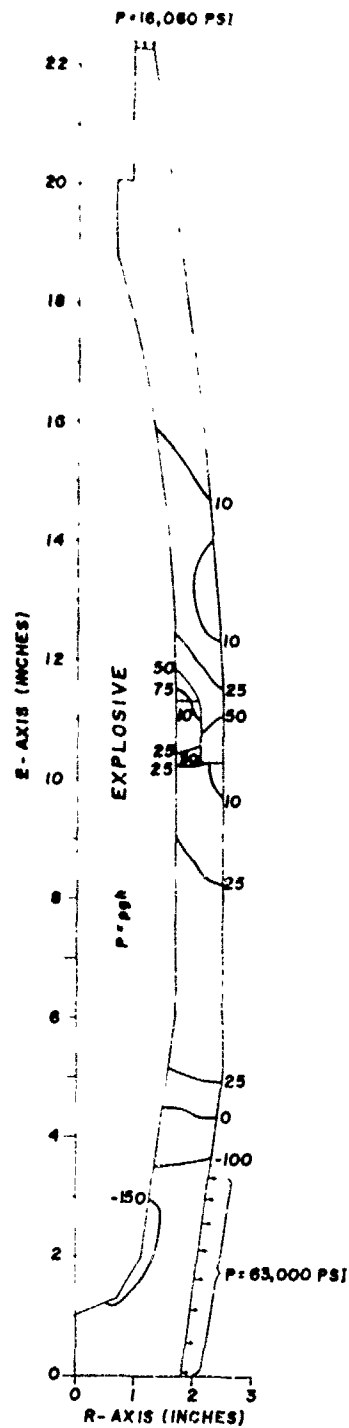


FIGURE 10. HOOP STRESS CONTOURS AT 18,000 g's ACCELERATION

VON MISES STRESS CONTOURS (KSI)

HI-FRAG INTERFERENCE FIT

ELASTIC ANALYSIS 18,000 g's

$\delta = .005"$

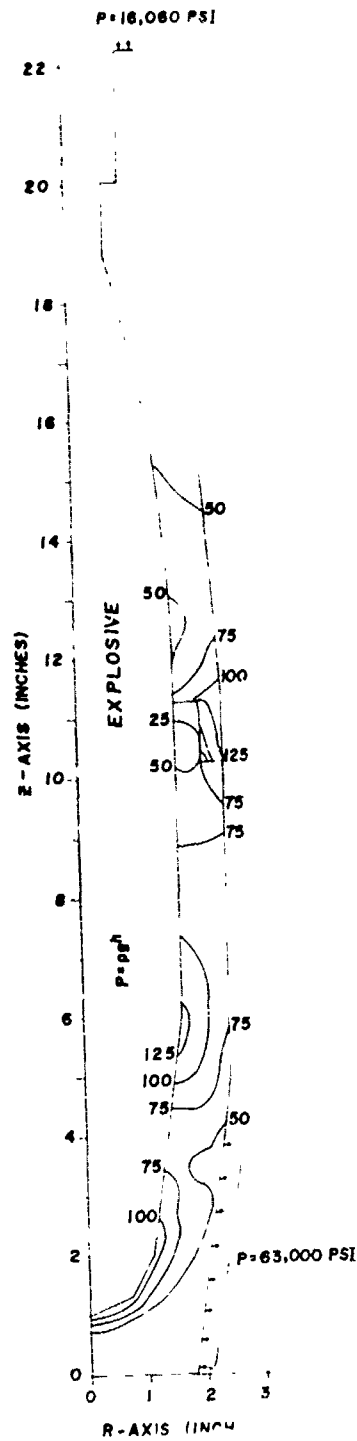


FIGURE II. VON MISES STRESS CONTOURS AT 18,000 g's ACCELERATION

VON MISES STRESS CONTOURS (KSI)

HI-FRAG JOINT MESH

ELASTIC ANALYSIS AT 18,000 g's.

$\delta = .006"$

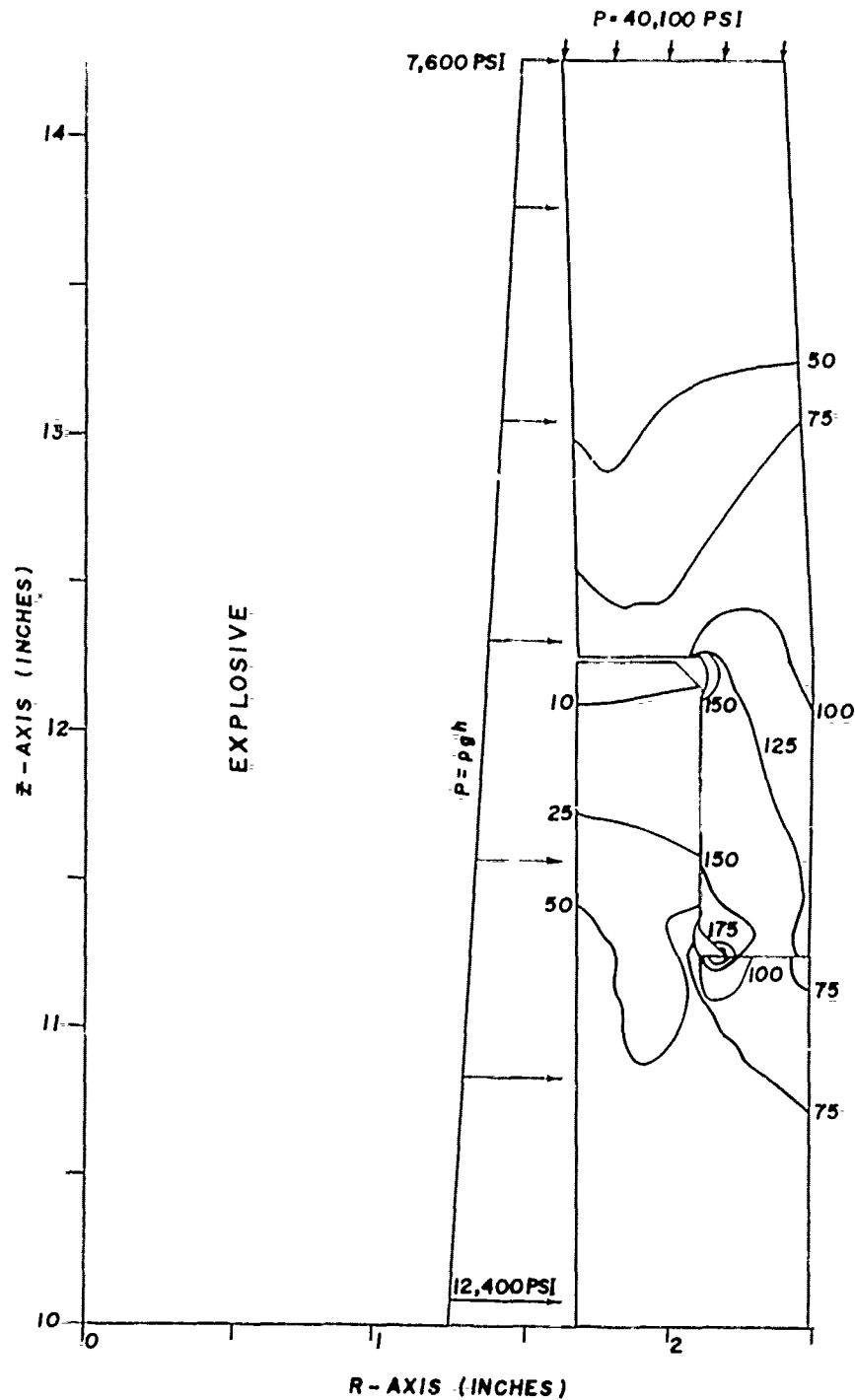


FIGURE 12. VON MISES STRESS CONTOURS FROM ELASTIC - ANALYSIS OF JOINT REGION AT 18,000 g's ACCELERATION

HOOP STRESS CONTOURS (KSI)

HI-FRAG JOINT MESH

ELASTIC ANALYSIS AT 18,000 g's

$\delta = .006''$

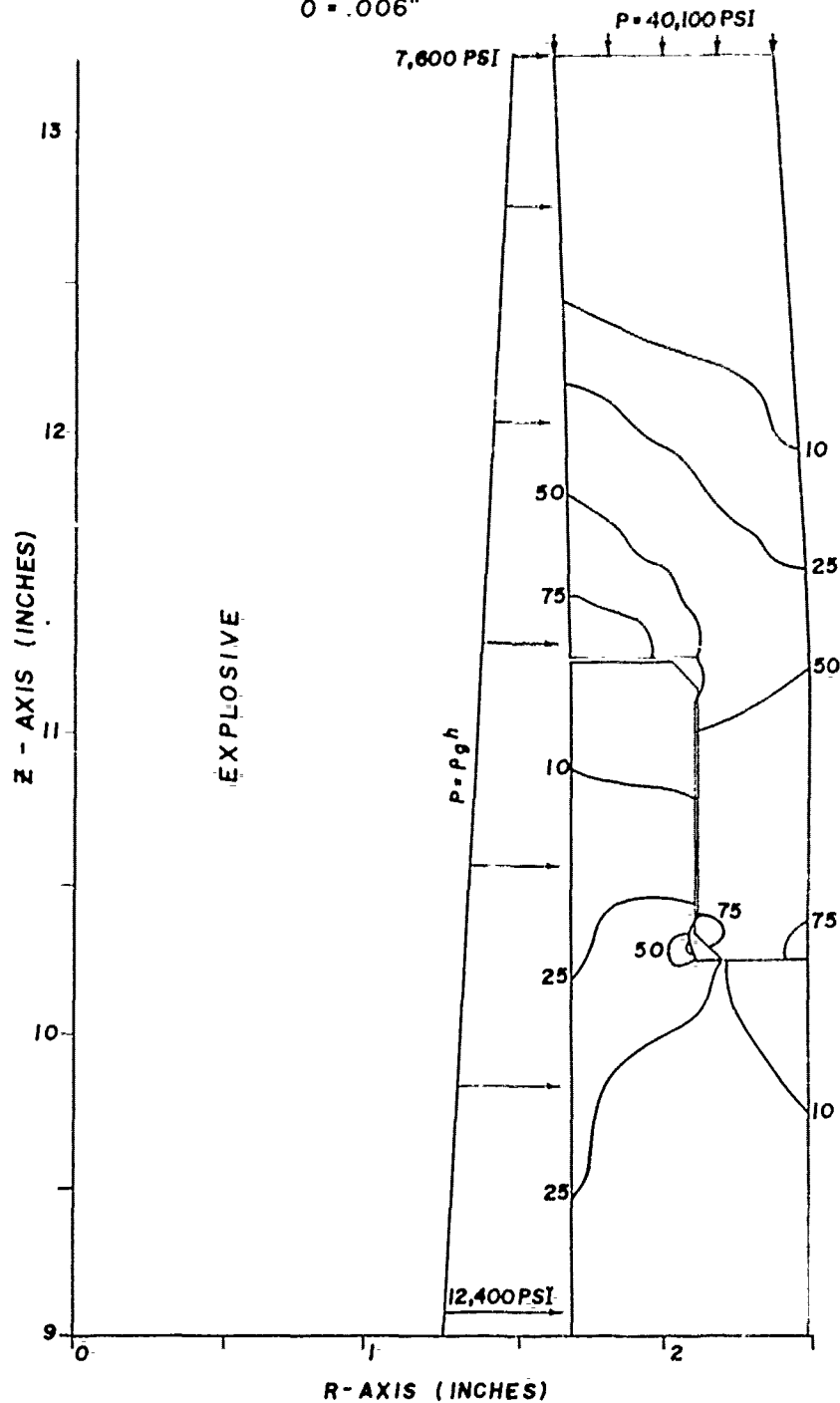


FIGURE 13. HOOP STRESS CONTOURS FROM ELASTIC ANALYSIS OF JOINT REGION AT 18,000 g's ACCELERATION

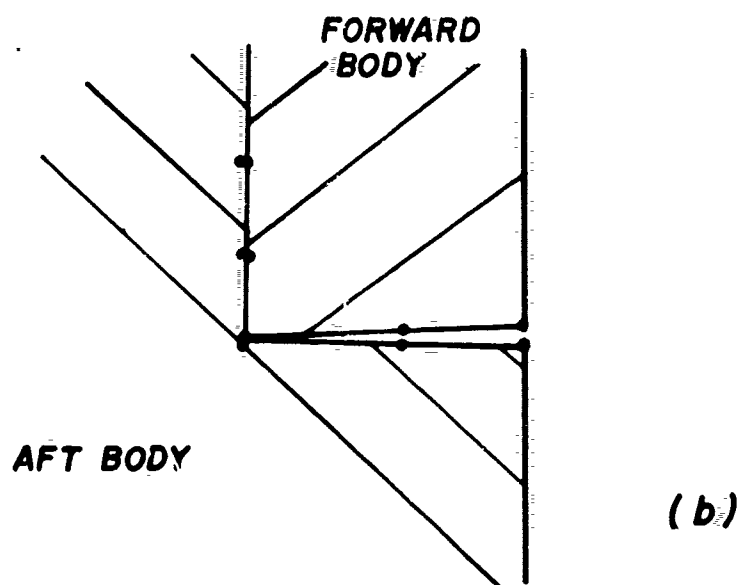
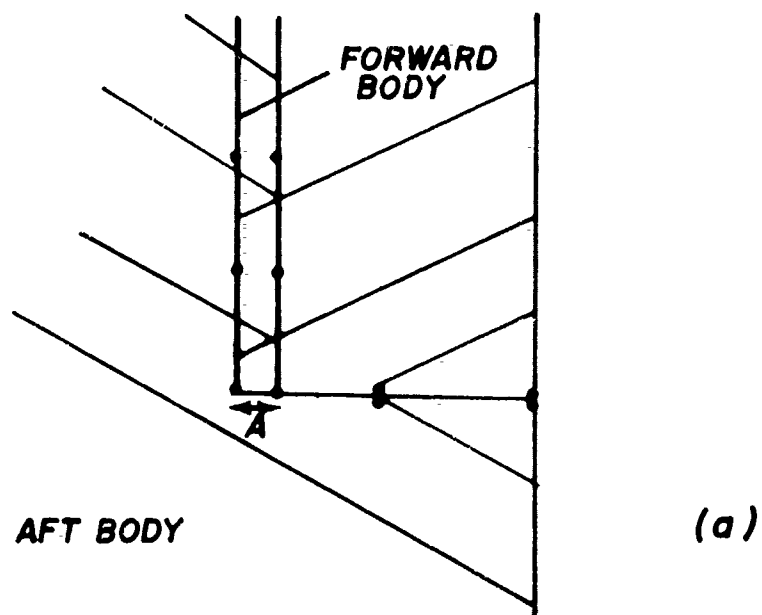


FIGURE 14. ADJOINING SURFACES WHICH ARE INITIALLY CLOSED (a) MAY GAP (b) WHEN INTERFERENCE IS REMOVED

Since the von Mises stress was well above the yield stress (150 KSI) an elastic plastic analysis was performed using the stress strain curve shown in Figure 4. This data was obtained at strain rates of 0.05 in/in/min. Its use in the present analysis in which the projectile is loaded at rates up to 5 in/in/sec should introduce only small errors in the result. In general, the yield stress will be slightly higher than the static value and the work hardening will be slightly less.

The results of the elastic plastic analysis for a 0.006 inch radial interference is given in Figures 15 and 16. The dotted sections on Figure 15 show the regions that yielded. This yielding in the joint region can significantly reduce the holding force of the joint after the setback loads are relaxed.

The hoop stress shown in Figure 16 has three places where it is above 75 KSI. At 0.006 inch interference the maximum hoop stress is located above the joint region on the interior surface of the nose. The hoop stress at this point is 90 KSI. The other two places are at the bottom of the joint in the nose. The section on the interference surface has a maximum of 87 KSI and the section of the outer surface has a maximum of 83 KSI.

During spin up the joint must transmit a torque to the nose and fuze. Appendix C treats this problem and shows that the interference fit is not able to transmit the required torque. Previous analyses, reference (7), based on engraving of the nose by the knurling in the base, do not appear to be applicable to the HI-FRAG design due to the very small amount of engraving in the joint surface.

However, the contact surface across which the axial load is transmitted can transmit a much larger torque than is required for spin up. Thus, the joint does not slip during spin up.

VON MISES STRESS CONTOURS (KSI)
 HI-FRAG JOINT MESH
 ELASTIC-PLASTIC ANALYSIS AT 18,000g's
 $\delta = .006"$

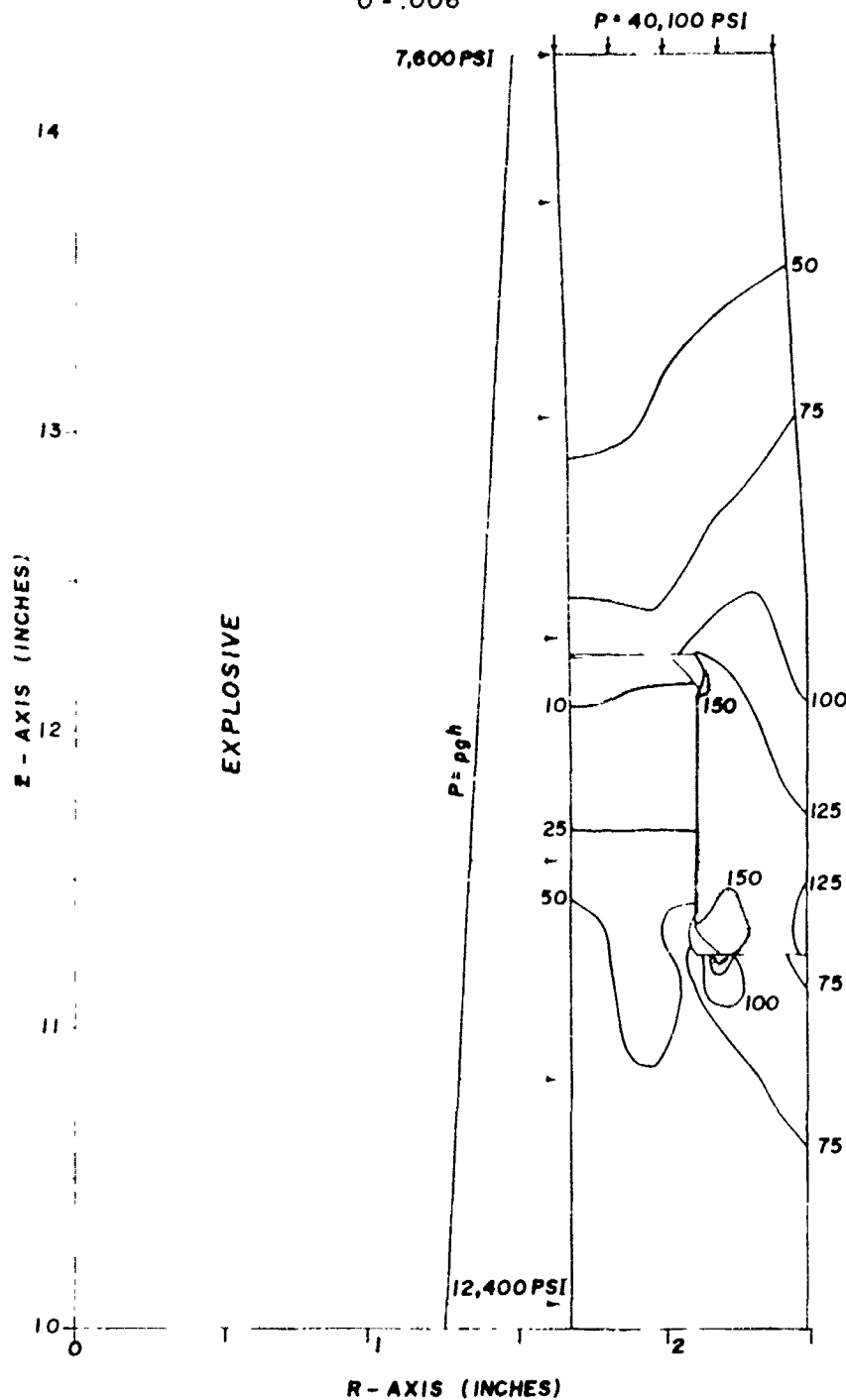


FIGURE 15. VON MISES STRESS CONTOURS FROM ELASTIC-PLASTIC ANALYSIS OF JOINT REGION AT 18,000g's ACCELERATION, DOTTED AREAS YIELD

HOOP STRESS CONTOURS (KSI)
HI-FRAG JOINT MESH
ELASTIC-PLASTIC ANALYSIS AT 18,000g's
 $\delta = .006"$

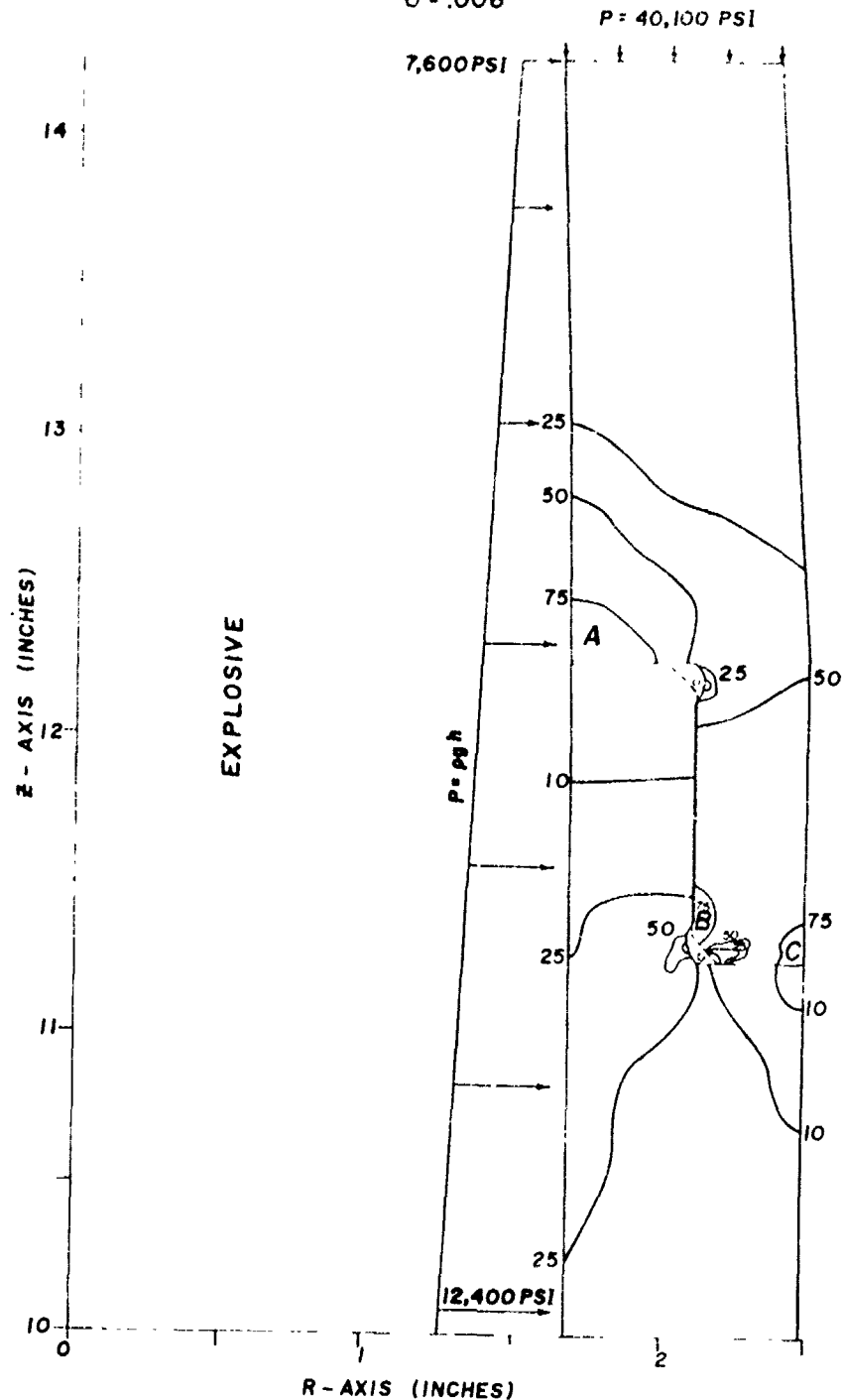


FIGURE 16. HOOP STRESS CONTOURS FROM ELASTIC-PLASTIC ANALYSIS OF JOINT REGION AT 18,000g's ACCELERATION

CRITICAL FLAW SIZE

The use of linear fracture mechanics in the evaluation of the critical flaw size for the 5"/54 HI-FRAG Projectile has proven extremely difficult. The various complicating factors are discussed below.

First, the material in the joint region is close to the yield point. Since critical flaw size calculations are based on the equations of elasticity with a small plastic zone correction factor, the accuracy of these results are dubious in region B of Figure 16. The results are regions A and C should be more accurate.

Second, the projectile is not in uniaxial tension and the crack tip is probably not in plane strain. The complex stress state greatly complicates the use of linear fracture mechanics theory. To obtain some degree of safety, the von Mises stress will be used to calculate the plastic zone correction factor. This is not rigorous, mathematically, but does cover the worst case.

Third, only a limited amount of longitudinal K_{IC} data is available for HF-1 steel at 150 KSI yield strength. However the transverse value of K_{IC} is required to predict crack propagation under a tensile hoop stress. No transverse K_{IC} data was obtained from projectiles machined from bar stock. The mass produced projectiles will be forged from bar stock. The difference in the methods of production can produce a difference in K_{IC} values.

Finally, the magnitude of the hoop stress is influenced by the radial pressure set up by the explosive at setback. A fluid model was used to calculate these pressures. No data is presently available to evaluate the use of this fluid model. Its justification consists of the low shear strength of PBXW-106 (about 40 psi) and the fact that it gives an upper limit to the actual pressure. If the explosive pressure is significantly less than the fluid model values, then the tensile hoop stress will also be less.

Keeping in mind this list of complicating factors, the critical flaw sizes are calculated as follows. A particular shape is assumed for the flaw, usually a sharp elliptical crack with a minor axis of a and a major axis of c . Then a flaw shape factor, Q , can be calculated from,

$$Q = \phi^2 - 0.212 \left(\frac{\sigma_{V.M.}}{\sigma_y} \right)^2$$

where

$$\phi = \int_0^{\pi/2} \sqrt{1 - \left| \frac{c^2 - a^2}{c^2} \right| \sin^2 z} dz = \text{complete elliptical integral of the second kind.}$$

σ_y = yield strength of HF-1 (150 KSI)
 $\sigma_{V.M.}$ = von Mises stress of the region without the flaw.

Note that the von Mises stress is used to calculate Q as was discussed above.

Since a surface flaw is more severe than an embedded flaw, the case of the surface flaw will be considered. The critical minor axis (a_{cr}) under a tensile stress, σ , is given by

$$a_{cr} = \frac{Q}{1.21} \left(\frac{K_{IC}}{\sigma} \right)^2$$

where K_{IC} = plane strain critical fracture toughness 31.4 KSI $\sqrt{\text{in}}$
 σ = maximum tensile hoop stress.

Using this equation, the dimensions of critical flaws can be determined. For a 0.006 inch radial interference at 18,000 g's, the critical flaws for the three regions (A,B,C) of high tensile stress are shown in Figure 17. The numerical values of a_{cr} for surface flaws in these three regions at $a/2c$ ratios of 0.5, 0.1, and 0 are given in Table I. To determine the radius of embedded cracks merely multiply the surface flaw a_{cr} by 1.21.

The worst orientation for this flaw is such that it appears on the surface as a long thin longitudinal crack. Upon sectioning the projectile wall, the elliptical geometry can be observed (Figure 17).

The maximum tensile hoop stress in the base was about 60 KSI. The associated critical flaw sizes are also shown in Table I. This work is currently being extended to cover a range of interferences and a range of accelerations.

The use of a plate equation for critical flaw size in a cylindrical specimen required some discussion. Based on the analysis presented in reference (11) the error in neglecting the cylindrical geometry is less than 0.5% for flaws having a_{cr} less than 0.1 inches. Thus, the use of the above equation appears justified.

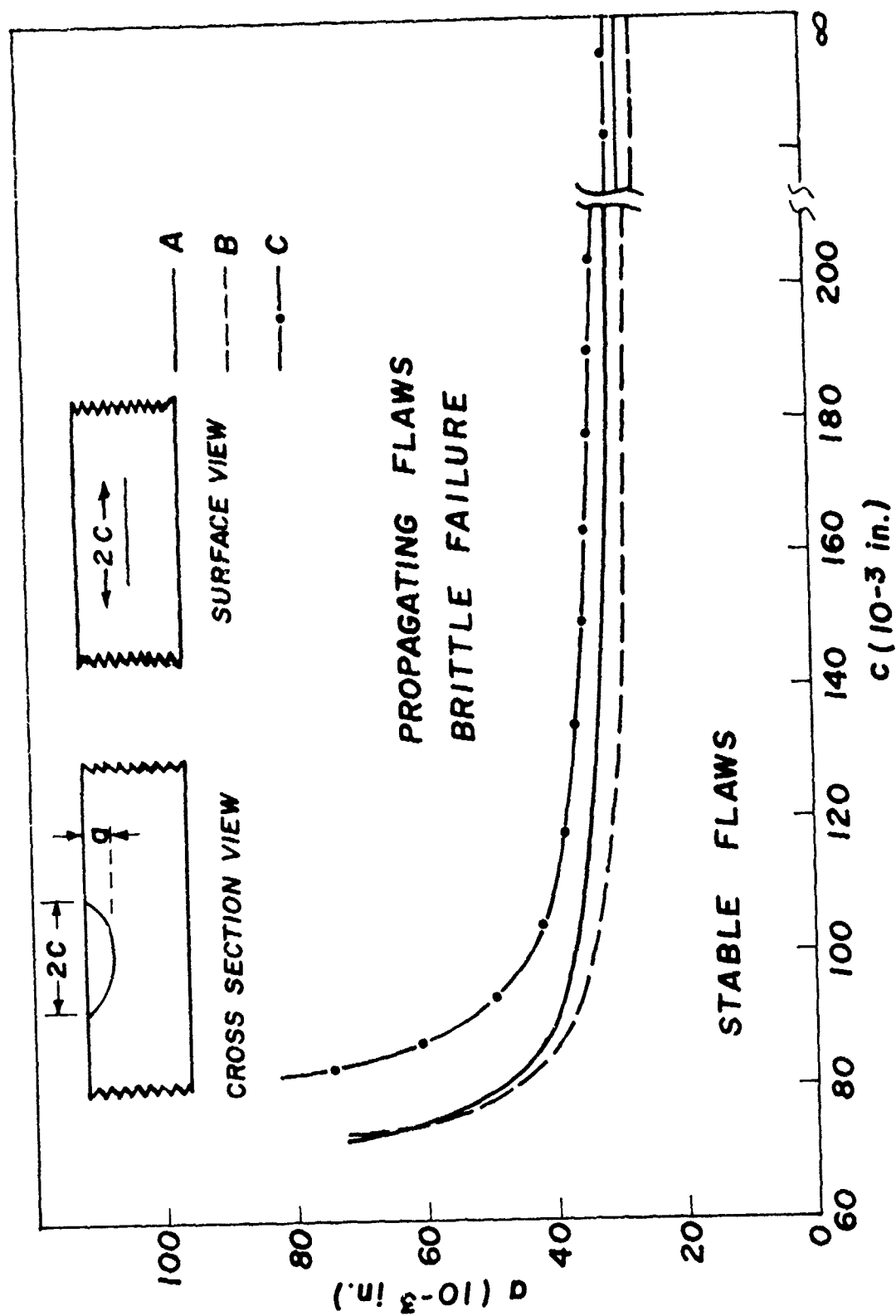


FIGURE 17. CRITICAL FLAW SIZES FOR REGIONS A, B, C SHOWN IN FIGURE 16

TABLE I
CRITICAL SURFACE FLAW DIMENSION
AT .006 RADIAL INTERFERENCE

<u>Region</u>	<u>σ_{HOOP} (KSI)</u>	<u>a/2c</u>	<u>a_{cr} (in.)</u>
A	90	0.5	.072
		0.1	.032
		0	.028
B	87	0.5	.073
		0.1	.029
		0	.026
C	83	0.5	.082
		0.1	.034
		0	.030
BASE	60	0.5	.167
		0.1	.074
		0	.066

REBOUND

As the projectile leaves the barrel the axial acceleration drops from 2,500 g's to zero in a very short interval of time (about 300 microseconds). This releases the stored elastic energy in the projectile in the form of sonic waves causing the projectile to ring at its natural frequency (4400 hertz). This phenomenon is called rebound.

This ringing effect can in no way change the rigid body motion of the projectile. The accelerations that are quoted from dynamic finite element analyses of rebound are particle accelerations that last about one-fourth of the natural period of the projectile (6×10^{-5} seconds). Due to this very short duration, rebound will have very little effect on the joint in the HI-FRAG Projectile.

However, concurrent with rebound is a large change in the aerodynamic effects on the projectile. As the projectile emerges from the barrel, an aerodynamic drag is exerted on the projectile. If all of this drag is exerted on the nose the joint is in compression and no problems will occur. If most of the drag is exerted on the base, then the joint is in tension and slippage may occur.

Moore, et al. , reference (12), have calculated the 5"/54 muzzle blast and post ejection environment of the projectile. An extension of this work should provide the necessary details to determine if these aerodynamic forces can cause slippage of the joint.

DISCUSSION

If natural high fragmentation is the major objective of the HI-FRAG Program, then a brittle material such as HF-1 steel is required. However, to then choose a design such that this material is placed in tension (residual stresses due to press fit) is, from a structural point of view, a paradox. If both a brittle material and a press fit are design requirements then one must pay a penalty in high quality control.

The analysis suffers from two uncertainties: the explosive pressure on setback and the effect of knurling on the interfaces. Both of these uncertainties can be removed through further testing.

A projectile instrumented with piezoelectric pressure gages should be able to measure the explosive pressure on setback. This type of test is necessary to truly characterize PBXW-106.

From the limited amount of testing shown in Appendix A, the press fit in the 5"/54 IMPROVED Projectile presents a large scatter in the data. This may in part be due to the behavior of the knurling. No comparable data is presently available for the HI-FRAG Projectile. Due to the higher yield strength of the HI-FRAG steel (150 KSI versus 80 KSI) one might expect the knurling in the HI-FRAG Projectile to yield much less than in the IMPROVED Projectile.

If this is the case, then both an upper and lower limit on the interference after knurling should be specified in the contract. At present, only before-knurled dimensions are specified. The lower limit could be set by the minimum holding force required for the joint. The upper limit could be set by critical flaw size considerations.

Besides limiting the interference after knurling, it would be of some benefit to taper the knurling on the interference surface. Since the hoop stress is largest at the bottom of the joint, a reduction in the interference in this region could substantially increase the critical flaw size in the joint itself. However, it would have little effect on the critical flaw size just above the joint (region A on Figure 16).

Next, consider the effect of knurling on the contact surface which transmits the axial loads. The purpose of the knurling is to distribute the loading evenly across the surface. The analysis showed that variations on the order of .0005 inches can cause a large stress concentration if both surfaces have high yield stresses. Assuming that the knurling conforms to the surface of the nose then these concentrations are avoided.

The effectiveness of the knurling in distributing the axial load should be tested in the lab. The proper combination of strain

gages and extensometers should provide the necessary data.

It has been suggested that the knurling on this contact face could be replaced by a soft thin metal washer. This should also be able to relieve any axial stress concentrations. The washer will attempt to extrude upon setback which may present some design problems. However, these could be experimentally evaluated by a few tests.

Since this contact surface must transmit the torque required for spin up, the metal washer must have a high enough coefficient of friction to be able to transmit this load. This will require a certain surface roughness on the nose, base, and washer surfaces.

For various reasons such as corrosion, it would be beneficial to have the washer made of the same basic material as the projectile. Thus, a mild steel would appear to be a possible candidate.

The present HI-FRAG design may have a temperature problem. At 160°F the interference has decreased by at least .0004 inches. This variation can easily be taken into design consideration. However, under misfire conditions (Appendix A), the interference may decrease by .003 inches. This is much harder to include in the initial design. This problem will require some attention before the projectile design is fixed.

The major problem in the present design is the large tensile stresses set up by a press fit. This leads directly to the problem of the small critical flaw size.

A possible design alternative to the press joint is an adhesive joint. The present design contains 9.6 in² of interference surface. The holding force in the present design has a minimum value of about 14,000 lbs. This is the equivalent to a shear strength of about 1,500 psi.

The joint experiences a large quantity of shock and vibration loading. Thus, the adhesive will need to be tough.

Many adhesives require a thermal cure. The possibility of raising PBXW-106 to 200 or 250°F is not an attractive one but it still exists as a possibility. However, prudence would dictate the use of a room temperature cure adhesive if at all possible.

Once cured, the adhesive must retain its strength after many temperature cycles from -60°F to +160°F. It also must be able to maintain some strength at +400°F for 10 minutes.

Since projectiles can have shelf lives on the order of 20 years, the adhesive must be able to maintain its strength over this time frame. The joint must be impervious to environmental effects for the same period of time.

At present, the author is not convinced that an adhesive exists which can meet all of these requirements. Rowe, reference (13), has suggested Anaerobic adhesives as a candidate. Based on the data given in reference (14), Anaerobic adhesives have shear strengths up to 6,000 psi, can withstand large vibrations, are impervious to normal liquids encountered in machinery cooling or lubrication, and can be obtained to withstand 400°F up to 10 hours. Data on the mechanical properties of these adhesives is available only over a one year period; however, at the end of the year, the adhesive joint is still increasing in strength.

If the proper adhesive can be found, the payoffs should be very large. An adhesive joint does not place a residual tensile stress on the nose. A tensile hoop stress will be set up at gun launch but its value will be much less than in the present design. This will greatly increase the critical flaw size for the projectile. Moreover, the cost of the overall round should be reduced. The knurling on the press fit surface could be eliminated completely. The quality control problem of detecting extremely small flaws would be removed but the problem of examining the quality of the adhesive joint would replace it.

If tests show that adhesives cannot meet all the requirements, then a combination press fit adhesive joint is another possibility. One could possibly obtain the same strengths from the joint at a much lower interference. This is also one possible means of overcoming the temperature problem associated with a hangfire.

CONCLUSIONS AND RECOMMENDATIONS

The conclusions, based on results of this study, are as follows:

1. The critical flaw size for the HI-FRAG Projectile with HF-1 steel varies with interference. At .006 inches radial interference, a_{cr} is .026 for the worst type of flaw.
2. The interference decreases as temperature increases. Under mis-fire conditions this may present some difficulties.
3. Limits on the after knurled interference should be specified.
4. The press fit cannot transmit the required torque for spin up at 18,000 g's. However, the adjacent contact surface should easily be able to transmit the necessary torque.
5. Rebound will not cause the joint to slip. However, the aerodynamic forces associated with the exit of the projectile out of the barrel may cause some problems.

The recommendations are as follows:

1. Behavior of PBXW-106 explosive on setback should be more thoroughly defined by analytical and experimental studies.
2. Lab tests should be conducted on the HI-FRAG joint to determine the effect of knurling on both surfaces.
3. A more detailed study of HF-1 steel should be performed. In particular, the stress strain curve at 5 in/in/sec should be obtained along with K_{IC} data at different temperatures.
4. The possibility of replacing the knurling with a soft metal washer shows some merit. This possibility could be evaluated by lab tests.
5. The possibility of replacing the press fit with an adhesive joint should be considered. Lab tests could be used for a preliminary evaluation of an adhesive joint.

REFERENCES

- (1) NWL Technical Report TR-3148, "Finite Element Computer Program for the Solution of Nonlinear Axisymmetric Contact Problems with Interference Fits", Jun 74.
- (2) NWL Technical Note TN-E-2/74, "Finite Element Stress Analysis of the 5"/54 High Fragmentation Projectile Using ZP26 Computer Code", Jan 74.
- (3) H. Stordahl and H. Christensen, "Experiences From Stress Analysis of Axisymmetric Problems in Machine Design," in Finite Element Methods in Stress Analysis, ed. by Holland and Bell, 1970.
- (4) NWL Technical Note TN-E-18/74, "Assurance of an Adequate Joint Fit Of 2-Piece Projectiles", Dec 73.
- (5) NWL Technical Report - to be published, "Material Selection and Evaluation For the 5"/54 HI-FRAG Projectile", Confidential.
- (6) John Thompson - private communication, Jun 74.
- (7) NWL Technical Note, TN-E-9/72, "Stress Analysis of the Improved 5"/54 Projectile Press-Fit Joint", Jul 72
- (8) O. Hörger, and C. Nelson, "Design of Press- and Shrink-Fitted Assemblies", Journal of Applied Mechanics, Mar 73, A-32.
- (9) O. H. Griffin, NWL Memo, "Stress Analysis on a Retaining Ring", Dec 8, 71.
- (10) NWL Technical Report, TR-2624, "Investigation of 5" Gun In-Bore Ammunition Malfunctions", Dec 71.
- (11) E. Folias, "Axial Crack in a Pressurized Cylindrical Shell", International Journal of Fracture Mechanics, 1, 2, Jun 65. 104-113.
- (12) NWL Technical Report, TR-3000, "Calculation of 5"/54 Muzzle Blast and Post Ejection Environment on Projectile", Jan 73.
- (13) E. Rowe, private communication, Jun 74.
- (14) Handbook of Adhesive Bonding, ed. by C. Cagle, McGraw-Hill Book Co., New York, 1973.
- (15) E. Volterra, and J. Gaines, Advanced Strength of Materials, Prentice-Hall Inc., Englewood Cliffs, N.J., 1971.

(16) NWL Technical Report TR-3087, "The Thermal Environment of the 5"/54 Gun Barrel and Ammunition", Feb 74.

(17) K. Symon, Mechanics, Addison-Wesley Publishing Co., Reading, Mass., 1964.

(18) J. Faupel, Engineering Design, John Wiley and Sons, Inc., New York, 1964.

(19) O. Griffin, NWL Memo, "Experimental Measurements of Non-Metallic Discarding Rotating Band Pressures", Aug 25, 72.

APPENDIX A

THE EVALUATION OF KNURLING AND HOLDING FORCE OF PRESS FIT JOINTS

The ability of a press fit joint to transmit axial and circumferential loads is directly proportional to the interference pressure. Thus, a press fit should be designed such that the interference pressure is large enough to transmit the required loads while keeping the induced residual stresses small enough so that material failure is not encountered.

If yielding occurs in the joint, only a limited amount of interference pressure can be obtained. Since one of the interference surfaces is knurled, it is important to quantitatively determine the stresses which the knurling can support. To evaluate the effect of the knurling, several projectiles instrumented with strain gages were pressed together in the lab. These measured values of strain were then compared to the computer results. Since the computer model does not include the effects of knurling, the difference in the computed and measured values should be attributed to the knurling.

A strain gage (gage 1) was placed on the outer surface of the nose piece of five 5"/54 IMPROVED Projectiles. These gages were located 0.5 inches above the base (Figure A-2). Two additional gages were placed on one of these noses. One of these gages (gage 2) was located on the outer surface at the very bottom of the joint. The other gage (gage 3) was mounted on the inner surface just above the joint. All gages measured hoop strain.

These noses were then pressed onto bases giving a range of interference values. The hoop strains for gage one are plotted versus radial interference on Figure A-1. Also shown is the computer results for the hoop strain at this location.

As can be seen, the data has a slight tendency to fall below the computer prediction indicating small scale yielding. However, in general, the discrepancies between the predicted values and the measured values is less than 15%.

The data for the nose instrumented with three strain gages is given in Figure A-2 along with the computer predictions for each location. As expected, the largest variation occurred for gage 2 which is located at the bottom of the nose. This may indicate partial yielding of the knurling at the stress concentration region near the bottom of the interference fit. It may also indicate uneven wearing down of the knurls due to several assemblies and disassemblies.

In general, the computer model provides excellent predictions for the upper limit of the measured hoop strains. Even though the knurling has a tendency to yield, its behavior often approaches that of a solid

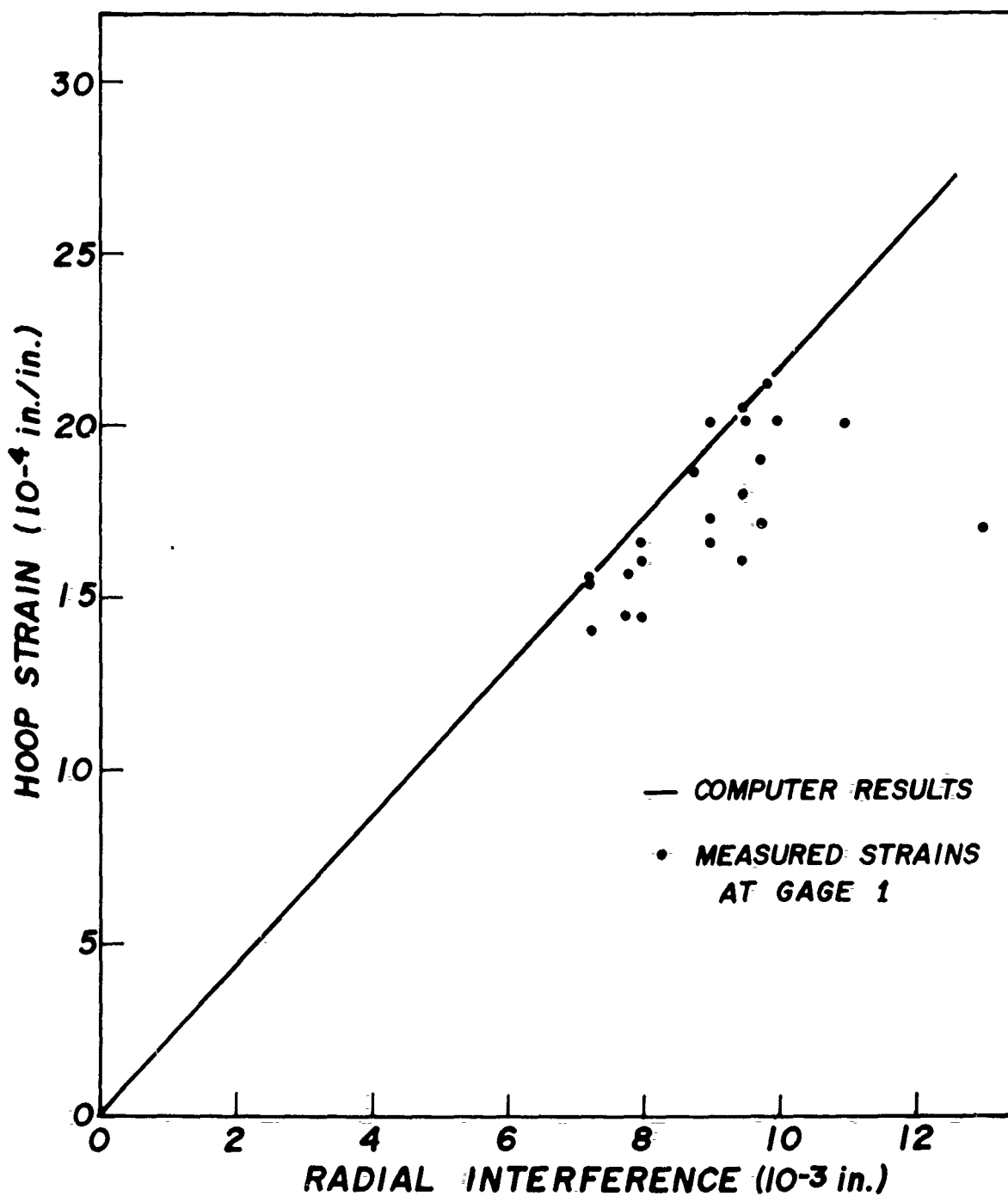


FIGURE A-1. MEASURED HOOP STRAIN VERSUS RADIAL INTERFERENCE ON 5"/54 IMPROVED PROJECTILES

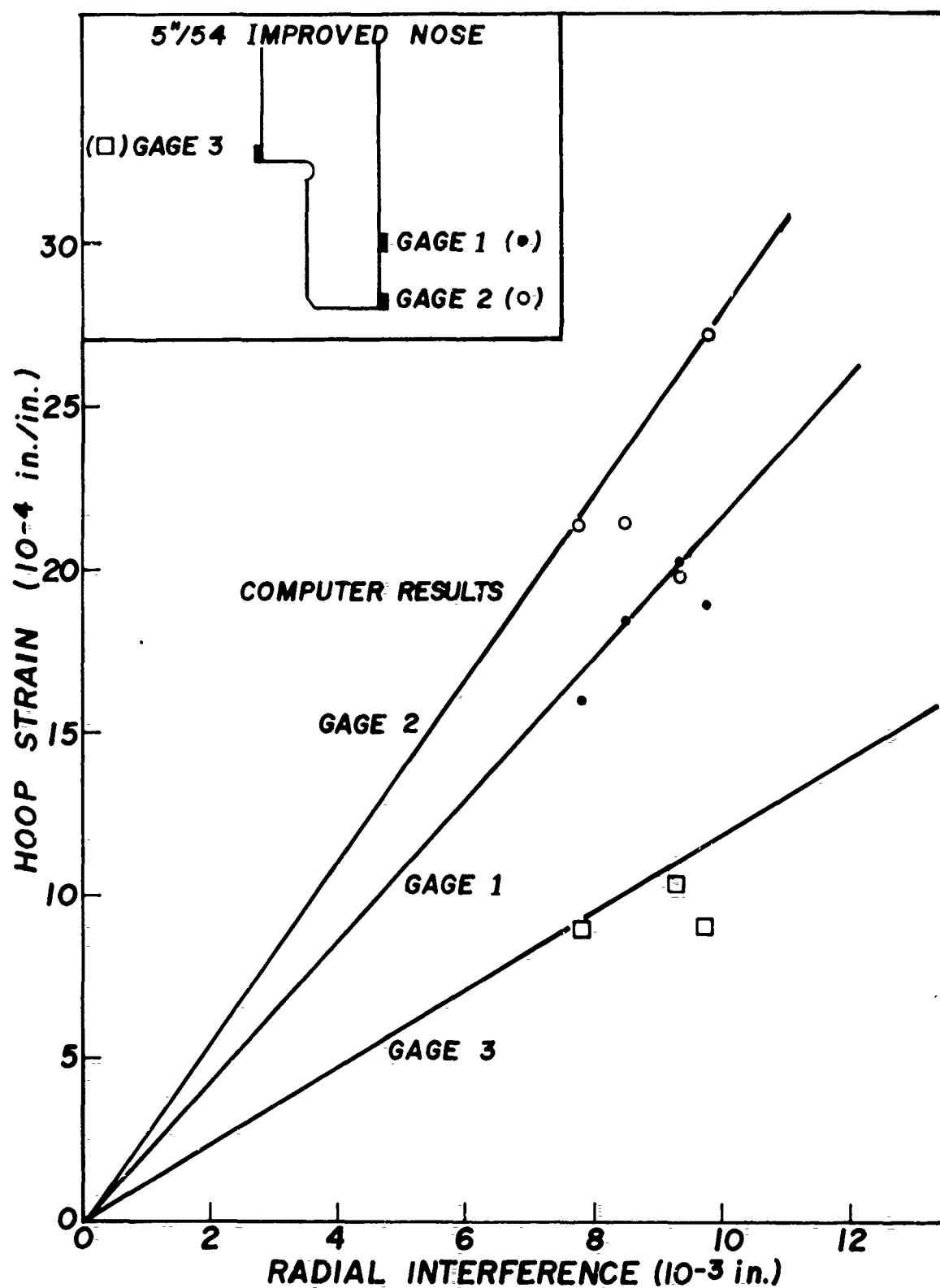


FIGURE A-2. MEASURED HOOP STRAIN VERSUS RADIAL INTERFERENCE AT 3 LOCATIONS ON 5"/54 IMPROVED PROJECTILES

surface. Thus, the computer results must be considered as the worst case or upper limit of the stress state under any given loading condition.

The holding force of the joint was obtained by measuring the axial force required to initiate slip in the joint. These loads are plotted versus radial interference in Figure A-3. At least squares fit was performed on the data with the constraint that the holding force must be zero at zero interference. This yields the function

$$F = 2.64\delta$$

where F = holding force (KIPS)
 δ = radial interference (10^{-3} inches)

The interference stress obtained from the computer analysis on the IMPROVED Projectile was integrated over the interference surface to obtain the normal force. This normal force was then multiplied by the coefficient of static friction (μ) to obtain a computer estimate of the holding force. Horger et al. (8) report an average value of μ of 0.15. This gives a holding force of

$$F = 2.54\delta$$

Once again, the model has provided excellent results.

The interference pressures for both 5"/54 IMPROVED and HI-FRAG are shown in Figure A-4 at 0.006 inches radial interference. The similarity is quite apparent. The computer model predicts a holding force for the HI-FRAG Projectile of

$$F = 2.80\delta$$

The holding force is a function of temperature. Thus, it is necessary to consider the change in holding force over the temperature range the projectile will see.

The change in radial dimensions (u) as a function of temperature is given by

$$u = r\epsilon_{\theta} + r\alpha T$$

where r = radius
 ϵ_{θ} = hoop strain
 α = linear coefficient of thermal expansion ($6.5 \times 10^{-6}/^{\circ}\text{F}$)
 T = temperature difference from room temperature (70°F).

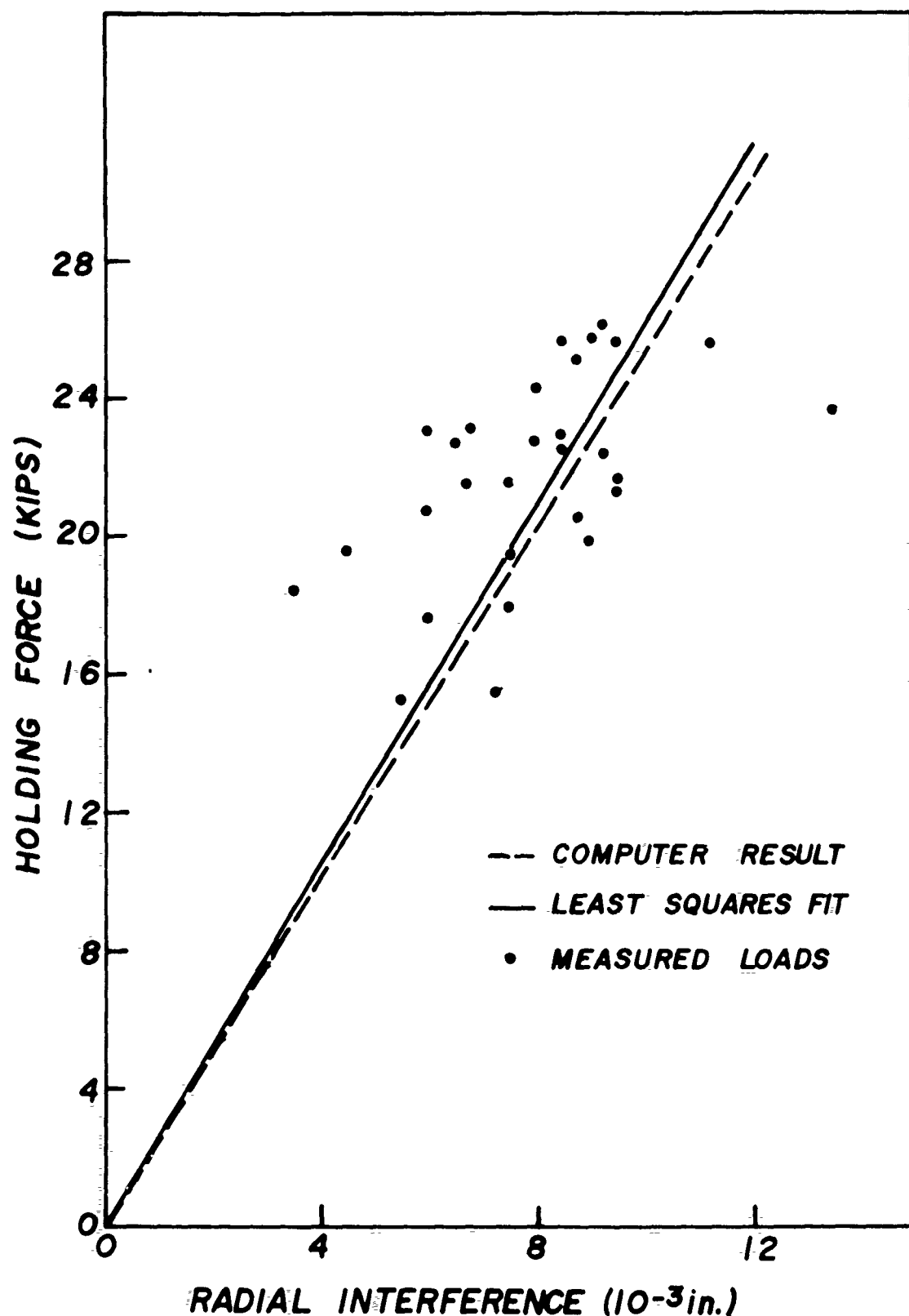
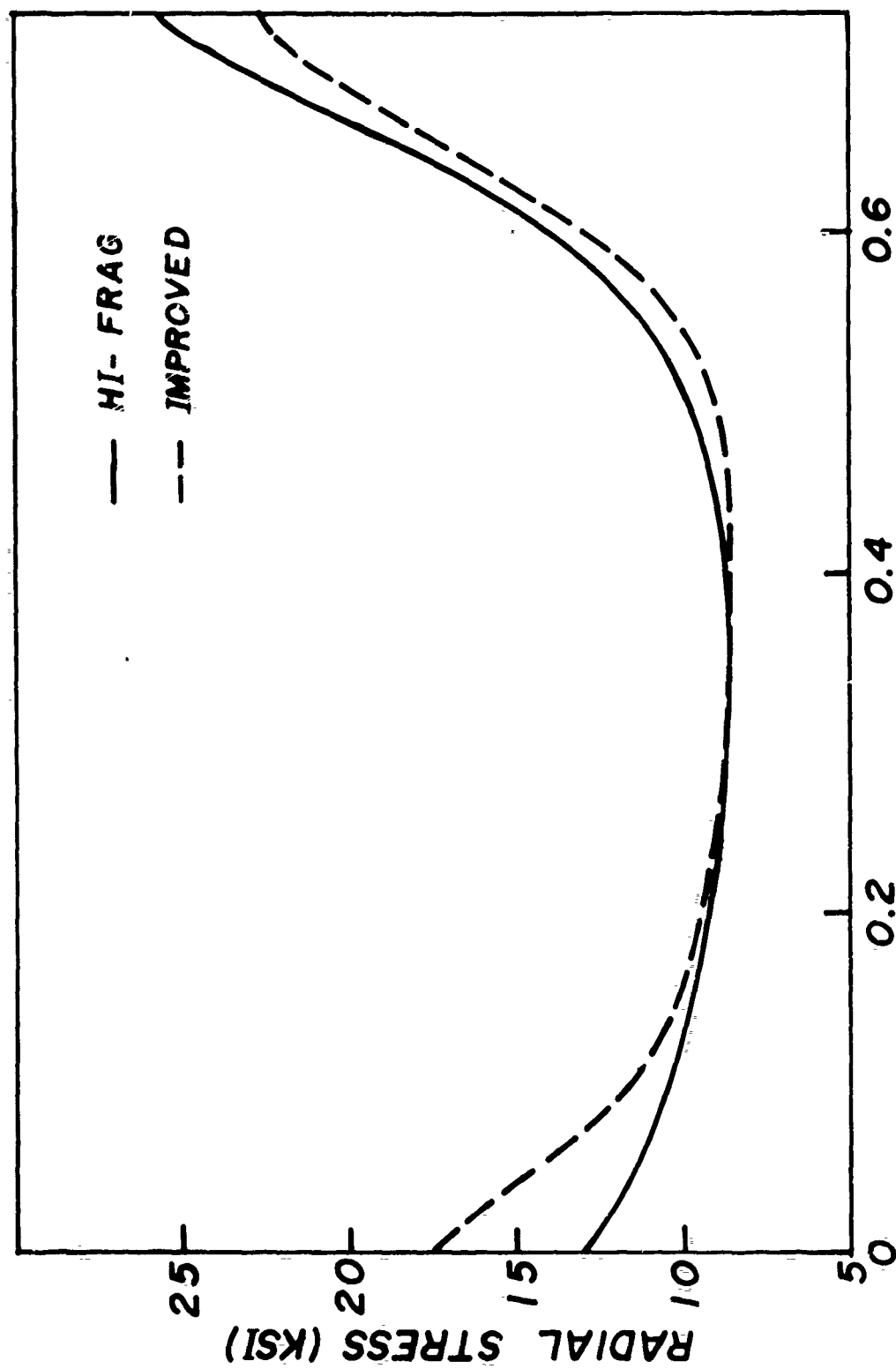


FIGURE A-3. MEASURED HOLDING FORCE VERSUS RADIAL INTERFERENCE FOR 5/54 IMPROVED PROJECTILE, ALONG WITH COMPUTER PREDICTION



DISTANCE ALONG INTERFACE (inches)

FIGURE A-4. COMPARISON OF INTERFERENCE PRESSURE DISTRIBUTION FOR THE HI-FRAG AND IMPROVED PROJECTILES

Reference (15) shows that this can be expressed as

$$u = \alpha r \left[\frac{(1+\nu)}{r^2} \int_{R_i}^{R_o} T r dr + \frac{(1-\nu)}{R_o^2 - R_i^2} \int_{R_i}^{R_o} T r dr + \frac{(1+\nu) R_i^2}{(R_o^2 - R_i^2) r^2} \int_{R_i}^{R_o} T r dr \right]$$

Assuming a constant temperature distribution, this reduces to

$$u = \alpha r \left[(1+\nu) T \frac{R_o^2 - R_i^2}{2r^2} + \frac{(1-\nu) T}{2} + \frac{(1+\nu) R_i^2 T}{2r^2} \right]$$

The change in interference for the HI-FRAG Projectile is given by the difference in the radial deformation of the outer cylinder and the radial deformation of the inner cylinder at the press fit. This is given by

$$\begin{aligned} \Delta \delta &= u_i - u_o \\ &= -3.4 \times 10^{-6} T \end{aligned}$$

The range of temperatures at which the projectile is tested is -60°F to +160°F. Since the holding force is measured at 70°F, T varies from -130°F to +90°F and the radial interference varies ±0.0004 inches. This is a negligible error at the higher interferences, but may play a role if the interference is less than .003 inches.

A slightly different case may arise in the case of a malfunction. Present Navy procedure in the case of a misfire allows the projectile to remain in a hot barrel for a period of 10 minutes maximum before firing. Reference (16) shows that the inside of the projectile could reach temperatures on the order of 300°F and the outer part of the projectile on the order of 400°F. Using these values, the change in interference is about .003 inches. Thus, the true interference if the projectile is fired in this configuration, is .003 inches less than the interference at 70°F. This may present a very serious problem for projectiles having initial interferences less than .005 inches.

APPENDIX B

DYNAMIC EFFECTS AT GUNLAUNCH

It is necessary to determine the accuracy of a static stress analysis in obtaining the stress state under gunlaunch conditions. If the error due to dynamic effects is large, a static analysis provides meaningless results.

Consider the projectile as a simple linear system. Its natural frequency can be approximated by dividing the sound speed of the material (16,800 ft/sec) by twice its length (23 in.).

$$f = 4400 \text{ hertz}$$

This method obtains good estimates (within 0.5%) of measured values for projectile body natural frequencies (10).

Next, consider the frequency of the forcing functions. This can be estimated from the inbore acceleration time curve (Figure B-1). An exact analysis would consist of decomposing this curve into its various frequency components using a Fourier Integral. However, Figure B-1 shows that near peak acceleration, this curve can be approximated by a half sine wave with frequency of 56 hertz.

The error analysis is performed by comparing the dynamic solution of a linear system with a natural frequency of 4400 hertz driven by a 56 hertz sinusoidal force to the static solution. The equation of motion is given by Symon (17) as:

$$m\ddot{x} + b\dot{x} + kx = F_0 \sin \omega t$$

where x = the displacement
 m = the mass
 b = viscous force
 k = spring constant
 F_0 = magnitude of the driving force
 ω = frequency of driving force (radians/sec)

The dots indicate derivative with respect to time. The solution for our application is given by

$$x_D = -\frac{\omega F_0}{\omega_0^2 m} \frac{1}{\omega_0^2 - \omega^2} e^{-\gamma t} \sin \omega_0 t + \frac{F_0/m}{[(\omega_0^2 - \omega^2)^2 + 4\gamma^2 \omega^2]^{1/2}} \sin \omega t$$

where γ = damping factor ($\gamma = \omega_0$ is critically damped)
 $\omega_0 = \frac{\text{natural angular frequency of system (27,650 radians/sec)}}{\sqrt{k/m}}$

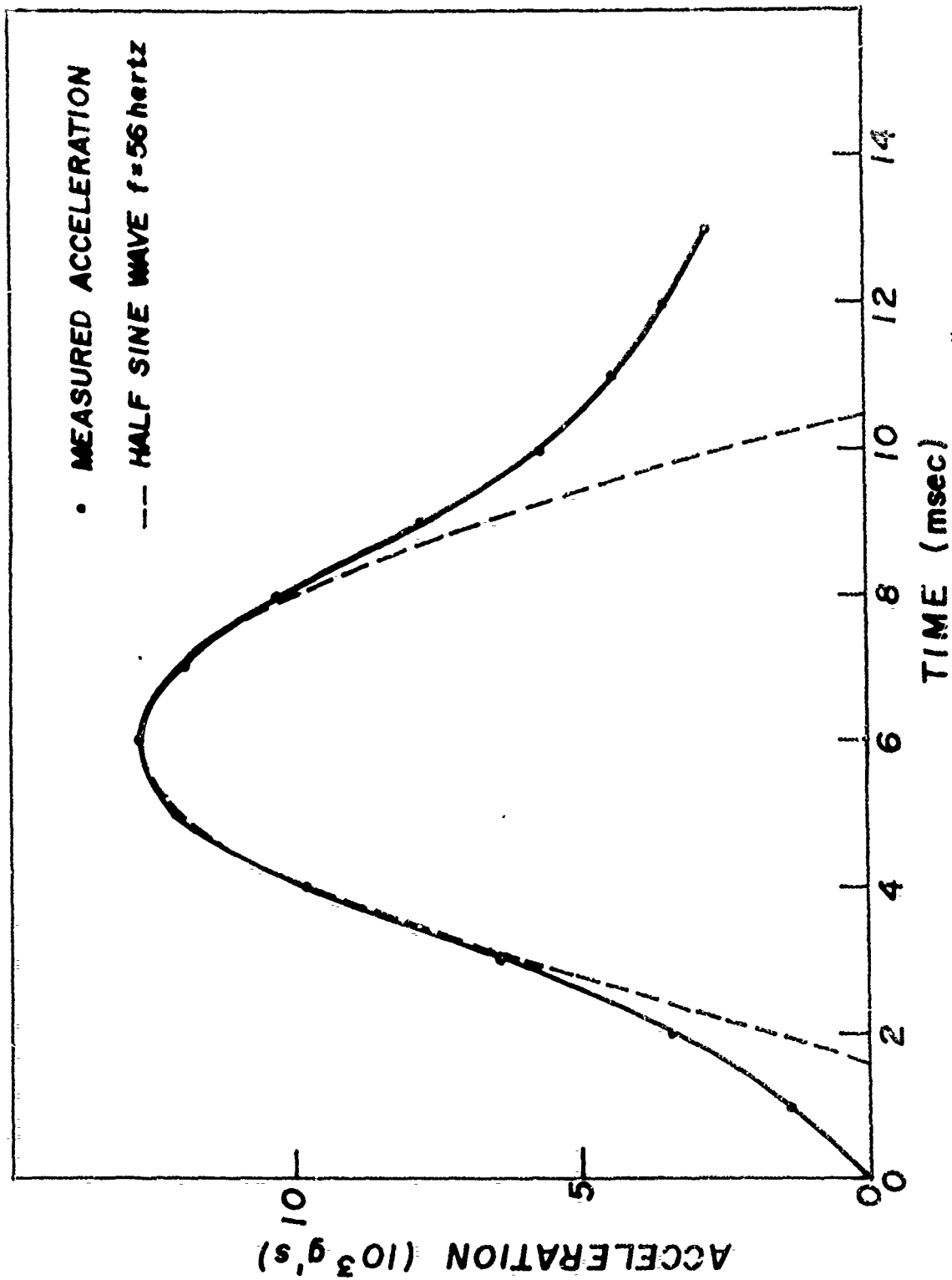


FIGURE B-1. TYPICAL ACCELERATION TIME CURVE FOR THE 5"/54 HI-FRAG PROJECTILE

The first term is the transient term which decays with time. The second term is the steady state solution.

This solution corresponds to the dynamic solution. A static solution is obtained by ignoring the first two terms in the equation of motion.

$$kx = F_0 \sin \omega t$$

The solution is

$$x_s = \frac{F_0}{m\omega_0^2} \sin \omega t$$

The relative error is obtained by dividing the difference of the dynamic solution and the static solution by the static solution.

$$R.E. = \frac{x_D - x_s}{x_s}$$

Reference (10) gives a γ of .02 ω_0 for the 5"/38 MARK 52 Projectile. Using this value and evaluating the relative error at maximum acceleration ($\sin \omega t = 1$) one obtains an error of .1%. Thus, the static solution should provide excellent results in this analysis.

From the data obtained on instrumented 5"/38 projectiles, it appears that there is a large shock component for some propelling charges. Most of these very high frequency components appear to decay within a 2 msec time interval. Thus, they should have a negligible effect on stress state at peak acceleration (6 msec).

A further source of dynamic loading is the side slap of the projectile against the bore. Since no data is available on this type of loading its effects are unknown.

APPENDIX C

ROTATIONAL EFFECTS AT GUNLAUNCH

A 5"/54 Projectile is spin stabilized. Thus, during gunlaunch various rotational effects contribute to the stress state of the projectile. Due to limitations in the computer program, these rotational effects are not included in the stress analysis. These effects are considered in this section and estimates of the errors associated with the neglect of these effects are made.

In general, the projectile rotation has two effects on the present analysis:

- a) Angular acceleration and angular velocity set up body forces which are not included in the computer results. These body forces not only change the stress state but also change the interference.
- b) The joint must transmit a torque to the nose section in order to avoid slippage between the two pieces during spin-up.

Consider the magnitude of the body forces. If no slippage occurs then the angular acceleration is proportional to the axial acceleration. Since the barrel is rifled at 125 inches/turn, the proportionality constant is given by

$$\dot{\omega} = 2\pi \frac{32 \times 12}{125} a = 19.3a$$

where $\dot{\omega}$ = angular acceleration (radians/sec²), and
a = axial acceleration (g's)

The body force due to this angular acceleration is given by

$$F_1 = r\rho\dot{\omega}$$

where ρ = mass density

r = moment arm

F_1 = body force due to angular acceleration.

The body force due to angular velocity is given by

$$F_2 = r\rho\omega^2$$

where ω = angular velocity

F_2 = body force due to angular velocity

The body force due to axial acceleration is given by

$$F_3 = \rho a$$

where F_3 = body force due to axial acceleration.

At 18,000 g's, $\dot{\omega} = 350,000$ radians/sec², and $\omega = 1100$ radians/sec.
This gives body forces of

$$\begin{aligned} F_1 &= 560 \text{ lbs/in}^3 \\ F_2 &= 1845 \text{ lbs/in}^3 \\ F_3 &= 5100 \text{ lbs/in}^3 \end{aligned}$$

This, however, is not a good method of evaluating the error in neglecting rotational body forces. Consider the effect of each force on the joint region. The axial force acts over a column length on the order of 10 inches. Thus, the axial pressure on the joint region due to the axial body force is about 51,000 lbs/in². The body force due to rotational velocity is in the radial direction and acts over the wall thickness (0.8 inches). Thus, the radial pressure due to rotational velocity is 1480 lbs/in². The body force due to angular acceleration is in the circumferential direction and is thus constant. Thus, the circumferential pressure is about 560 lbs/in².

The comparison of these pressures indicates that the error in neglecting the rotational forces is about 3%.

The angular velocity lowers the effective interference of the press fit by an amount, Δ (18), given by

$$\Delta = \frac{\rho c^2 \omega^2}{4E} (3+\nu) \left(1 - \frac{a^2}{c^2}\right)$$

where a = inside radius of base
 b = radius to press fit surface
 c = outer radius of nose
 ρ = mass density
 ω = angular velocity
 E = Young's Modulus
 ν = Poisson's Ratio

At 18,000 g's, this is a change of 0.001 inches. At 3,000 ft/sec muzzle velocity, the decrease in effective interference is 0.0003 inches. Thus, neither case gives an appreciable error.

The torque required to spin up the nose and fuze is given by

$$T = I\dot{\omega}$$

where T = torque
 I = moment of inertia of the nose and fuze (86.9 lb in²)

or

$$T = 4.36 a$$

where a = axial acceleration (g's)

At 18,000 g's, the required torque is 78,600 lb in. This torque is transmitted across two surfaces: the interference surface; and the contact surface which also transmits the axial loads.

Horger (8) gives a torsional coefficient of friction for press fits of about 0.25. Thus, the maximum torque which can be transmitted across the interference surface is obtained by multiplying the coefficient of friction, the total normal force, and the moment arm (2.115 inches).

At 18,000 g's and .006 inch radial interference, the normal force can be obtained from integrating the interference pressure across the surface (Figure 8). The maximum torque which can be transmitted across this surface is 51,900 lb in.

The normal force across the contact surface is given by the product of the weight of the nose and fuze and the axial acceleration.

$$F = 34.8 a$$

where F = normal force (lbs)

a = axial acceleration (g's)

The maximum torque which can be transmitted across this surface is the product of the normal force, the static coefficient of friction (0.15) and the moment arm (2.25 inches).

$$T = 11.7 a$$

Thus, at any given acceleration, this contact surface can easily transmit the required torque.

APPENDIX D

CONDITIONS DURING GUNLAUNCH

The loading conditions used in the computer model are as follows:

1. A rotating band pressure of 63,000 psi
2. A liquid model for the explosive PBXW-105 yielding a linear pressure distribution.

$$P = \rho gh$$

where ρ = explosive mass density (slugs/in³)
g = acceleration
h = distance from top of explosive

3. A fuze pressure of 16,060 psi based on a fuze weight of 2.08 lbs.

The third loading condition is a straight-forward calculation and requires no explanation.

The rotating band pressure for non-metallic bands has been measured at 33,000 psi at 12,000 g's acceleration, reference (19). In addition, a shear stress is exerted on the projectile by the rotating band. Using a more exact model for the rotating band actually lowers the stresses in the base of the projectile. Since this section will be shown not to be critically stressed, the less exact model was left in the analysis.

The explosive pressure, however, plays a very important role in the stress state of the joint. At present, no data is available on the explosive pressure of PBXW-106 at setback. Assuming that the explosive acts like a liquid probably yields an overestimate of the induced pressure. The larger this internal pressure is the larger the tensile hoop stresses set up in the projectile. Since the critical flaw size calculations are based on the tensile hoop stress the explosive pressure has a strong influence on the critical flaw size.

At present, there is no way to estimate the error involved in using a liquid model for the explosive.

APPENDIX E

DISTRIBUTION

Commander
Naval Sea Systems Command
Washington, D. C. 20360
Attn: SEA-04 (1)
SEA-048 (1)
SEA-049 (1)
SEA-03 (1)
SEA-0332 (1)
SEA-6531 (1)
SEA-6541 (1)
SEA-99 (1)
SEA-99 (Hawver) (1)

Defense Documentation Center
Cameron Station
Alexandria, Virginia 22314 (2)

Chief of Naval Operations
Department of the Navy
Washington, D. C. 20350 (1)

Commander
Naval Ordnance Laboratory
White Oak, Silver Spring, Maryland 20910
Attn: Code 702 (2)
Code 231 (2)
Code 412 (2)

Commander
Naval Weapons Center
China Lake, California 93555 (1)

Commanding Officer
Aberdeen Proving Ground
Aberdeen, Maryland 21005 (1)

Director
U.S. Army Ballistics Research Laboratories
Aberdeen Proving Ground, Maryland 21005 (1)

Director
Naval Ammunition Production Engineering Center
Naval Ammunition Depot
Crane, Indiana 47522
Attn: Code 04MB (1)

DISTRIBUTION (CONT'D)

Commanding Officer
Watervliet Arsenal
Watervliet, New York 12189
Attn: Dr. T. E. Davidson (1)

Commanding Officer
Naval Sea System Support Office Pacific
San Diego, California 92112 (1)

Commanding Officer
Naval Sea System Support Office Atlantic
Norfolk Naval Shipyard
Portsmouth, Virginia 23709 (1)

Commanding Officer
Frankford Arsenal
Philadelphia, Pennsylvania 19137
Attn: SARFA-PDM, H. Markus (1)
SARFA-PDME, J. Mulherin (1)
SARFA-PDME, Warren Ingliss (1)

Commanding General
Army Material and Mechanics Research Center
Watertown, Massachusetts 02172
Attn: Eng. Mech. Div., Paul Riffin (1)

Chief of Naval Material
Department of the Navy
Washington, D. C. 20360 (1)

Commanding Officer
Naval Weapons Station
Seal Beach, California 90740 (1)

Commanding Officer
Harry Diamond Laboratories
Washington, D. C. 20425 (1)

Commanding Officer
Army Weapons Command
Rock Island Arsenal
Rock Island, Illinois 61200
Attn: R&D (1)

DISTRIBUTION (CONT'D)

Commanding Officer
Navy Ships Parts Control Center
Mechanicsburg, Pennsylvania 17055 (1)

Commander
Naval Ordnance Station
Indian Head, Maryland 20640
Attn: ES43A (2)

Commanding Officer
Naval Ordnance Station
Louisville, Kentucky 40214 (1)

Commanding Officer
Naval Weapons Station
Yorktown, Virginia 23491
Attn: Code 64A (NEDED) (2)

Commanding Officer
Naval Weapons Station
Concord, California 94520
Attn: Code QEL (1)

Commanding Officer
Naval Ordnance Station
Forest Park, Illinois 60130 (1)

Commanding Officer
Picatinny Arsenal
Dover, New Jersey 07801
Attn: SMUPA-VAG (1)
SMUPA-VA (1)
SMUPA-DE (1)
G. Demitrak (1)

Commanding Officer
Naval Weapons Station
Charleston, South Carolina 29408 (1)

Commanding General
Army Material Command
Department of the Army
Washington, D. C. 20310 (1)

DISTRIBUTION (CONT'D)

Commander
Naval Safety Center
Naval Air Station
Norfolk, Virginia 23511 (1)

Director
Development Center
Marine Corps Development and Education Command
Quantico, Virginia 22134 (1)

Director of Naval Laboratories
Department of the Navy
Washington, D. C. 20360 (1)

Superintendent
Naval Academy
Annapolis, Maryland 21402 (1)

Commanding Officer
Army Research Office
Arlington, Virginia 22204 (1)

Commander
Naval Research Laboratory
Washington, D. C. 20390 (1)

Head
Mid Range Branch
Studies and Requirements Division
Development Center
Marine Corps Development and Educational Command
Quantico, Virginia 22134 (?)

UNCLASSIFIED

SECURITY CLASSIFICATION OF THIS PAGE (When Data Entered)

REPORT DOCUMENTATION PAGE		READ INSTRUCTIONS BEFORE COMPLETING FORM
1. REPORT NUMBER TR-3164	2. GOVT ACCESSION NO.	3. RECIPIENT'S CATALOG NUMBER
4. TITLE (and Subtitle) CRITICAL EVALUATION AND STRESS ANALYSIS OF THE 5"/54 HI-FRAG PROJECTILE		5. TYPE OF REPORT & PERIOD COVERED
		6. PERFORMING ORG. REPORT NUMBER
7. AUTHOR(s) Robert A. Londeman		8. CONTRACT OR GRANT NUMBER(s)
9. PERFORMING ORGANIZATION NAME AND ADDRESS Naval Weapons Laboratory Dahlgren, Va. 22448		10. PROGRAM ELEMENT, PROJECT, TASK AREA & WORK UNIT NUMBERS
11. CONTROLLING OFFICE NAME AND ADDRESS		12. REPORT DATE July 1974
		13. NUMBER OF PAGES
14. MONITORING AGENCY NAME & ADDRESS (if different from Controlling Office)		15. SECURITY CLASS. (of this report) UNCLASSIFIED
		15a. DECLASSIFICATION/DOWNGRADING SCHEDULE
16. DISTRIBUTION STATEMENT (of this Report) Distribution limited to U.S. Gov't agencies only; Test and Evaluation; (7-74).. Other requests for this document must be referred to the Commander, Naval Weapons Laboratory, Dahlgren, Va. 22448		
17. DISTRIBUTION STATEMENT (of the abstract entered in Block 20, if different from Report)		
18. SUPPLEMENTARY NOTES		
19. KEY WORDS (Continue on reverse side if necessary and identify by block number)		
20. ABSTRACT (Continue on reverse side if necessary and identify by block number) This report presents a detailed analysis of the loading conditions to which the 5"/54 HI-FRAG Projectile is subjected. These loading conditions include the following: press fit, gun ramming or rebound upon exit from the barrel. The analyses are based on finite element, analytical, and experimental results. Were applicable, various results are correlated to show their validity.		

DD FORM 1 JAN 73 1473

EDITION OF 1 NOV 65 IS OBSOLETE
S/N 0102-014-6601

UNCLASSIFIED

SECURITY CLASSIFICATION OF THIS PAGE (When Data Entered)

The analyses show that the joint region is the most highly stressed region in the projectile. The critical flaw size under 18,000 g's gunlaunch loading conditions is about 0.028 by 0.28 inches for a sharp elliptical crack in the joint region at 0.006 inches radial interference.

UNCLASSIFIED